Theses and Dissertations

2016

Nano Oil Additives And Their Effect On UH-60 Auxiliary Power Unit Performance

James Patrick Folk
University of South Carolina

Follow this and additional works at: http://scholarcommons.sc.edu/etd

Part of the Mechanical Engineering Commons

NANO OIL ADDITIVES AND THEIR EFFECT ON UH-60 AUXILIARY POWER UNIT PERFORMANCE

by

James Patrick Folk

Bachelor of Science
University of South Carolina, 2014

_____

Submitted in Partial Fulfillment of the Requirements

For the Degree of Master of Science in

Mechanical Engineering

College of Engineering and Computing

University of South Carolina

2016

Accepted by:

Abdel Bayoumi, Director of Thesis

Dale McCants, Reader

Lacy Ford, Senior Vice Provost and Dean of Graduate Studies

ACKNOWLEDGEMENTS

I would like to thank Dr. Abdel Bayoumi for providing me with the opportunity to perform research with CBM and for everything that he has done throughout my time in graduate school. I am grateful for all of the support from my family and friends throughout my college experience at USC. I would also like to thank Dr. Dale McCants for providing valuable suggestions while reviewing my thesis. I am also very thankful for all of the help and thesis recommendations provided by my friends and coworkers at CBM.

ABSTRACT

This study is designed to research the tribological properties of nano oils developed by NanoPro MT and to determine their effects on fuel consumption in an UH-60 Blackhawk Auxiliary Power Unit (APU). For this work, two different nano oils were tested and compared against the performance of conventional oil. The first nano oil mixture contains proprietary nanodiamond particles and the second nano oil contains a mix of zinc sulfide, boron nitride, and graphene particles. Aeroshell 560 was used as the conventional oil and was blended with the nano particles to create both nano oils. This oil meets the military specifications for use in the APU. The APU is part of a test stand that consists of a turbine engine, an APU Tester, an Electronic Sequencing Unit, a fuel tank, a fuel flow meter, a water brake dynamometer, and multiple other sensors. In addition to testing with the APU, the oils were tested in an AH-64 Apache Intermediate Gear Box (IGB). Testing was conducted on two separate test stands, one applying torque through an absorption motor and one where no torque load was applied. These tests provide additional data for determining the effects of friction by measuring vibration and temperature. Offline analyses were also performed to characterize additional oil properties. Knowledge of these properties was used while determining causes for the results of the other tests. Viscosity and particle size information is vital when forming conclusions about the thermal and tribological properties of the oils.

The research performed in this study utilizes data from each of these tests to characterize the oil and to summarize the advantages and disadvantages associated with the use of each oil. RStudio, Microsoft Excel, and Matlab were used to analyze the data and perform calculations. T-tests were used to determine the variance, margin of error, and percent error within individual runs. Analysis of Variance (ANOVA) and Tukey's Honest Significant Difference Test (HSD) were employed to compare results between runs. In all of the calculations a 95% confidence interval was used. The results of this study show that varying the concentration of nanoparticles in Aeroshell 560 turbine oil can drastically change the thermal properties of the oil. This research also suggests that Aeroshell 560 turbine oil containing zinc sulfide, boron nitride, and graphene particles can provide significant improvements in fuel efficiency and friction reduction. Oil containing nanodiamond particles also improves performance of the APU and IGB, but not to the same extent as the other nano oil. A small improvement in efficiency could result in millions of dollars of fuel savings for the U.S. Army if the oil is implemented fleet wide in the APU and even more if the idea is translated to the main power source of the aircraft, the T700 turbo jet engine.

TABLE OF CONTENTS

LIST OF TABLES

LIST OF FIGURES

LIST OF SYMBOLS

$\dot{W}$ Output power

$\dot{E}_{in}$ Energy input from fuel

$\dot{m}_{fuel}$ Mass flow rate of fuel

x Vibration data in a time domain

N Number of vibration data points

$\mathcal{W}$ Volumetric fuel flow rate

δ Ratio of measured barometric pressure to standard sea level barometric pressure

θ Ratio of measured ambient temperature to a standard temperature of 15°C

LIST OF ABBREVIATIONS

AED .... Aviation Engineering Directorate

ANOVA .... Analysis of Variance

APU.. Auxiliary Power Unit

CI.. Condition Indicator

DA1... Data Algorithm 1

ESU .... Electronic Sequence Unit

FFT.. Fast Fourier Transform

FM4..Fourth-Order Figure of Merit

HSD...Honest Significant Difference

IDB... Input Duplex Bearing

IGB.. Intermediate Gearbox

IRB .... Input Roller Bearing

MSPU... Modern Signal Processing Unit

ODB .... Output Duplex Bearing

ORB .... Output Roller Bearing

RMS ....Root Mean Square

STA... Synchronous Time Average

TEM .... Transmission Electron Microscope

TRDT .... Tail Rotor Drive Train

CHAPTER 1: INTRODUCTION

1.1 Background

  Lubricating oils serve several important purposes in mechanical systems. They are routinely used to reduce friction in bearings, gears, pistons, valves, and many other components. Excessive friction can result in decreased efficiency due to the loss of energy through heat, vibration, and the creation of wear. Ideally, the fluid film layer remains thick enough to separate mechanical components from making contact. For ball bearings, gear teeth, and other surfaces experiencing rolling contact the primary type of lubrication regime experienced is elastohydrodynamic. As the components get closer together, the oil between the surfaces begins to compress, but a fluid film will continue to provide a layer of separation between the surfaces. If this film is not sufficiently thick, boundary lubrication may occur. During the occurrence of this lubrication regime, the surfaces become close enough to partially contact each other, resulting in a significant increase in friction. Nanoparticle additives in the lubricant have been proposed to reduce contact between moving components. They act as extremely small ball bearings, which allow the materials to remain separated, thus reducing wear on the component surface. This study aims to determine the effects of graphene, zinc sulfide, boron nitride, and nanodiamond nanoparticles when used in the oil of an UH-60 Blackhawk auxiliary power unit (APU).

1.2 Literature Review

Numerous research projects have examined the properties of nano oils and have analyzed their impact on different mechanical systems. Lee et al. performed research on nano lubricants consisting of 0.1% and 0.5% graphite by volume. This study utilized a disk on disk tribotester to determine the effects on friction and wear. At 3000 N, the nano lubricant's friction coefficient was 24% lower than that of the base oil. The use of the nano lubricant also resulted in the temperature reducing from 116°C to 60°C. It was also determined that the addition of nanoparticles reduced wear and resulted in fewer surface scars[1].

Hadi and Mohamed analyzed graphite and zinc oxide nanoparticles suspended in engine oil. This research suggests that graphite particles are more effective than zinc oxide particles. It was determined that the graphite nano oil had a higher thermal conductivity and that the thermal conductivity increased as the concentration of graphite particles was increased. In addition to this result, the viscosity of the graphite nano oil was more stable over the range of temperatures at which it was tested. This research suggests that the higher concentration of graphite particles improved all tested properties of the lubricant[2]. While neither oil tested as part of the current study contains graphite, the research performed by Hadi and Mohamed demonstrates some of the benefits of using nano particles.

Gouda examined the application of boron nitride and graphite nanoparticles in gear and turbine lubricants. This study first examined the effects on common oil properties then compared temperature and vibration results during tests in an Apache IGB on the AH-64 Apache Tail Rotor Drive Train and No Load Test Stand. It was determined that both particles increased the thermal conductivity of turbine and gearbox lubricant and that the

2

thermal conductivity rose as the concentrations of particles were increased. For identical concentrations of nano particles, graphite resulted in a higher thermal conductivity. It was also observed that both particles increased the viscosity of the oils. The results from the No Load tests suggest that temperature and vibration continued to be reduced for concentrations up to 2% in gearbox lubricant. The 2.5% concentration caused an increase in temperature and vibration[3].

Nasiri-Khuzani et al. performed fuel consumption and wear tests in agricultural tractors running with nano diamond particles. These tests were conducted on eight Massey Ferguson Model 399 tractors with viscosity, fuel consumption, and additional variables being analyzed at 65, 90, 115, and 150 hours of run time. It was shown that viscosity was increased by the addition of nanoparticles. This research concluded that wear in cylinders, drive shafts, and gears was reduced by 68% while wear in rings and bearings was reduced by 64%. It also suggests that fuel consumption was reduced by 21%[4].

Fernandez studied power loss in bearings and gears. In this thesis, it was determined that the efficiency of a gearbox can be improved by modifying the oil. This study analyzes friction and viscosity of different oils and studies their effects on power loss in a wind turbine gearbox. It was found that oils with slightly higher viscosities improved the efficiency of gears, while the oils with slightly lower viscosities seemed to improve the performance of bearings[5].

1.3 Problem Definition

Lee et al., Hadi, and Mohamed perform valuable research which expands the current knowledge of nano lubricants and their basic properties. Gouda expands on this by

3

performing a more in depth study of these properties in addition to testing nano oils in actual military helicopter components. The fuel efficiency and wear research of Nasiri-Khuzani et al. is more similar to research performed as part of the current study. While these studies determine important properties of nano additives and suggest that there are substantial benefits to using nano oils, they do not analyze the effects of these additives in a turbine engine. The goal of this research is to further enhance the understanding of nano oil properties while determining any benefits associated with the use of nano particle oils in the UH-60 APU.   Based on the previous studies, reducing friction in the APU should reduce wear while improving fuel efficiency. Improving fuel efficiency and the rate of wear in the APU may result in large cost savings, if the proposed oil proves effective and is implemented across an entire fleet of aircraft. Wear reduction may also result in fewer component failures, which improves safety and reduces maintenance costs.

1.4 Problem Solution

The nano oil performance is compared using multiple tests to develop a more complete understanding of the effects of the particles in oil. Aeroshell 560 is used as the conventional oil as well as the base oil with which the nano particles are mixed to create the nano oils. It meets the military specifications for use in the APU. The exact compositions of nano particles in each oil is proprietary information and is not disclosed as part of this study. The lubricants are tested in the TRDT, No Load, and APU test stands. These test stands and the test procedures are explained in detail in Chapter 2. In addition to these tests, offline analyses are performed to provide a better understanding of the oils and their properties. Thermal and tribological properties including; friction, heat transfer,

4

viscosity, and particle size were analyzed in addition to fuel efficiency. The lubricant characteristics will be discussed and compared to those found in previous research and new findings for turbine effects are discussed. For this study, the oil containing nanodiamond is referred to as Batch A and the oil containing zinc sulfide, boron nitride, and graphene is Batch B.

CHAPTER 2: TEST STAND DESCRIPTIONS AND PROCEDURES

2.1 Tail Rotor Drive Train

2.1.1 Description of TRDT

The TRDT can be seen in Figure 2.1. It has been certified by The Aviation Engineering Directorate (AED) as sufficiently replicating flight conditions. It is composed of several AH-64 drive train components. The input motor is not shown in the image, but it rotates the #3 drive shaft which connects to the #4 drive shaft at the Forward Hanger Bearing. Drive shaft #4 connects to Drive Shaft #5 at the Aft Hanger Bearing. This shaft connects to the Intermediate Gearbox (IGB). Drive shaft #6 connects the IGB to the Tail Rotor Gearbox. Another motor, identical to the input motor, applies torque to the system. The absorption motor can apply 150% of the load that is created by the engines on the Apache and spins at 4,863 rpm, which matches the rpm experienced in flight.
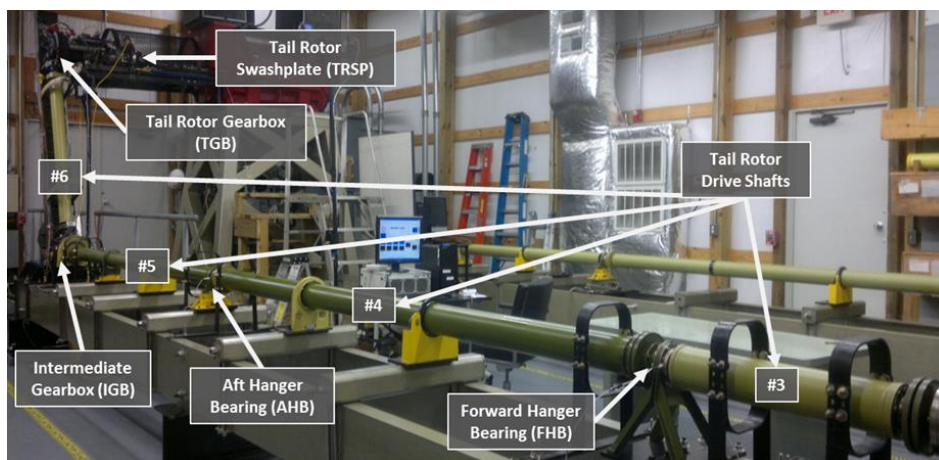
FIGURE 2.1 TAIL ROTOR DRIVE TRAIN TEST STAND

2.1.2 TRDT Test Procedure

The IGB was filled with 650 ml of conventional oil and installed on the TRDT. Twenty surveys were taken over five hours. This was performed five times to ensure that the data would be statistically significant. It was determined that all of the conventional oil could not be drained from the IGB without performing a change out. To prevent the inconsistencies associated with removing and reassembling components, 325 ml of conventional oil was removed using a pump and a concentrated Batch A.1 nano oil mixture was added. The one in Batch A.1 stands for the variation of that batch. For this work there are two iterations of Batch A. This oil was mixed with the remaining 325 ml of conventional oil to result in the desired concentration. The IGB was tested again for five hours, and repeated for five runs, with twenty surveys collected for each test. Then Batch A.1 nano oil and conventional oil results were compared. It should be noted that Batch B oil was not tested as part of this study. Batch B oil testing in the TRDT is detailed in the future work section of this document.

2.2 No Load Test Stand

2.2.1 Description of No Load stand

Figure 2.2 shows the No Load Test Stand. It is similar to the TRDT except that a torque load cannot be applied to the system. A five horsepower electric motor is used to spin the drive shafts instead of the 800 horsepower motor that is found on the TRDT. The No Load Test Stand can also be seen in the back of Figure 2.1. It is comprised of the same #3 through #5 drive shafts, hanger bearings, and IGB that are found on the TRDT. It does not have a #6 driveshaft, Tail Rotor Gearbox, or Output Motor. It can test components at the full operating speed of 4,863rpm while using far less power. This makes initial testing

much cheaper while still providing valuable data. The IGB is equipped with four thermocouples. The temperature can be measured at the Input Roller Bearing (IRB), Input Duplex Bearing (IDB), Output Roller Bearing (ORB), and the Output Duplex Bearing (ODB). These thermocouples are shown in Figure 2.3.
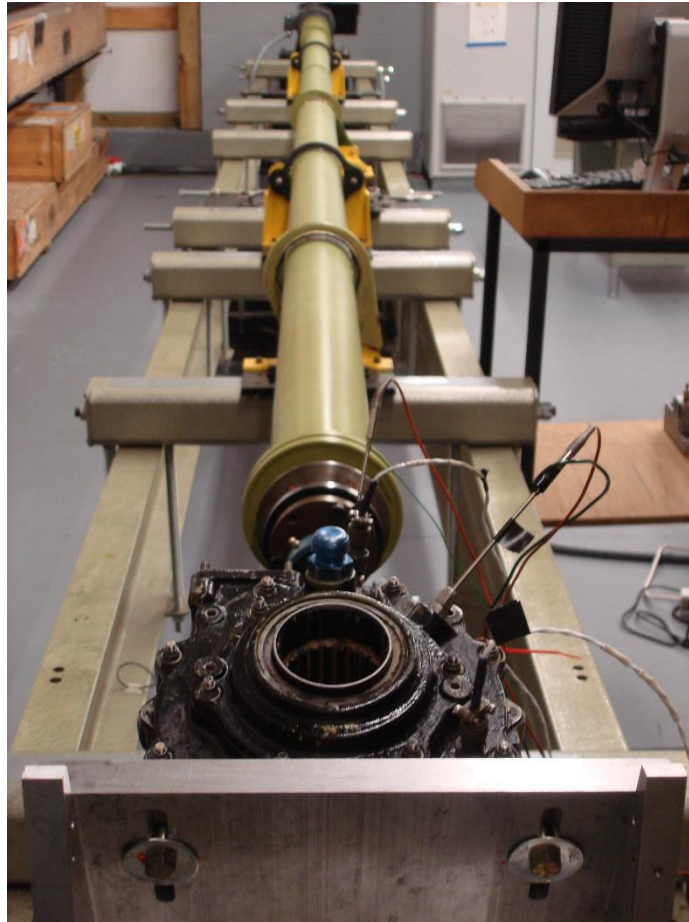
FIGURE 2.2 NO LOAD TEST STAND
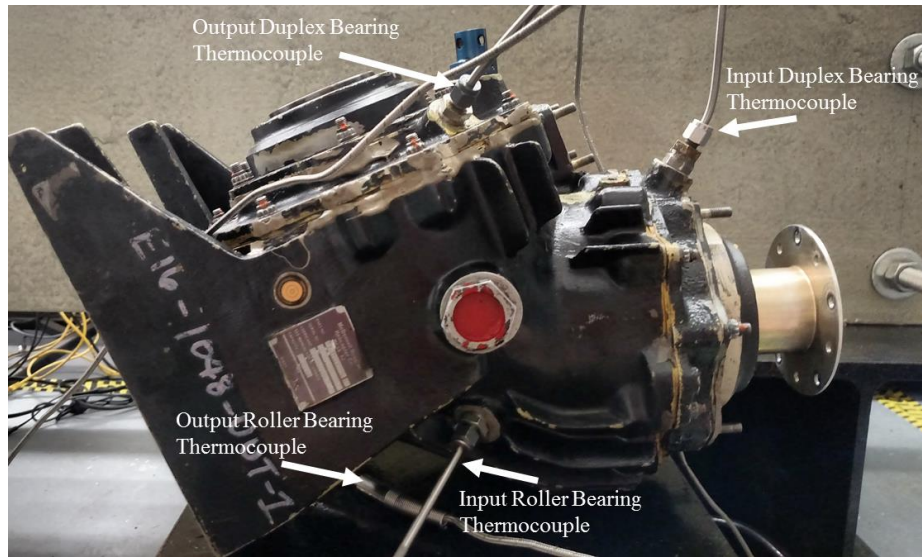
FIGURE 2.3 IGB THERMOCOUPLES

2.2.2 No Load Test Procedure

Four runs with conventional oil were performed to get baseline data. After this, Batch A.2, a higher concentration version of Batch A.1, was tested. It should be noted that multiple concentrations of Batch B were also tested. The tested oils include: Conventional, Batch A.2, Batch B.1, Batch B.2, and Batch B.3. All oils were tested four times, and each run lasted for 50 minutes. The drive shaft operated at 4,863 rpm and the test stand was assembled exactly the same way for every run to reduce the effect of external variables. The only source of data collected for this test was temperature measured at each of the bearings. The IGB was flushed multiple times with conventional oil between each run to remove any left over nanoparticles.

2.3 Auxiliary Power Unit Test Stand

2.3.1 Description of APU Test Stand
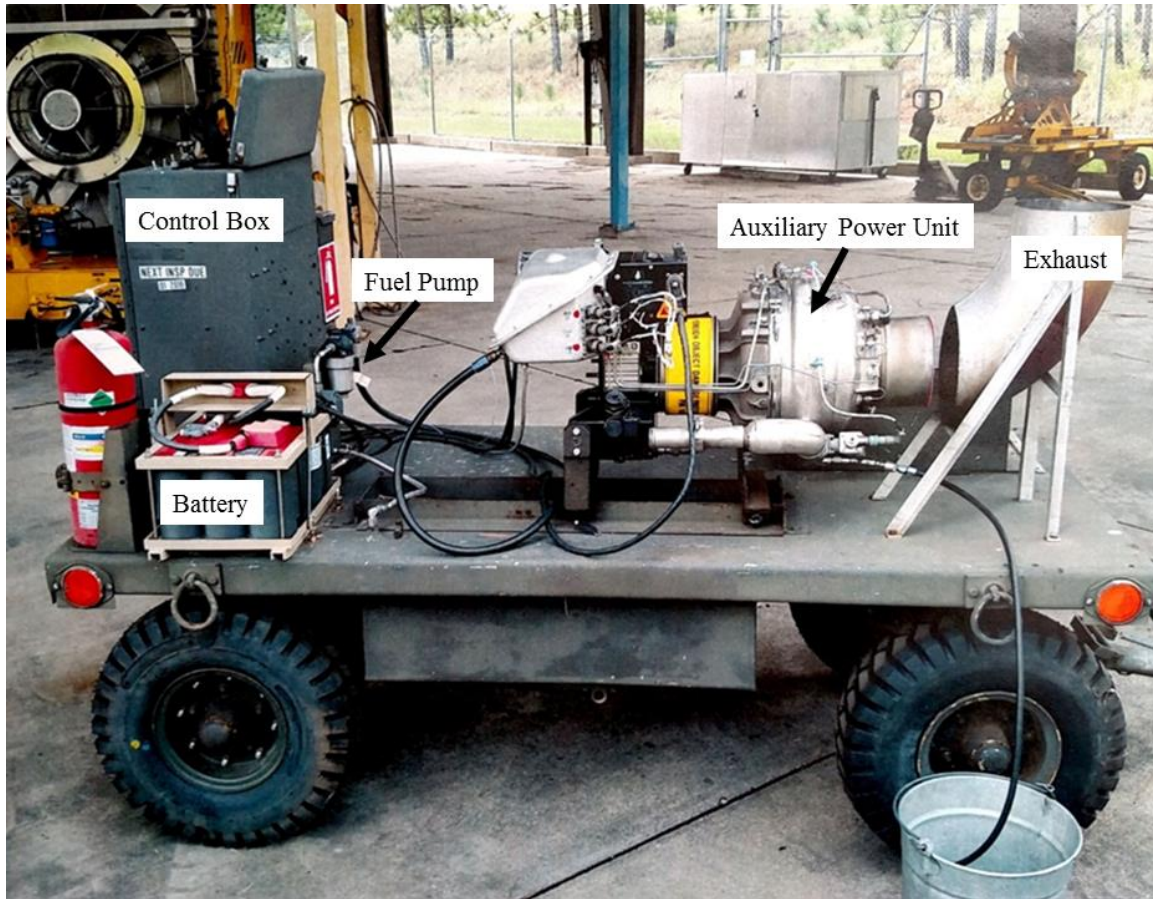
FIGURE 2.4 APU TEST STAND

Figure 2.4 shows the APU Test Stand. The battery, control box, and fuel pump can be seen on the left side of the image. The APU is near the center of the image, while the fuel flow meter, the remote servo control, the extended exhaust, and the water brake dynamometer are not shown in this picture.

The system operates by the fuel boost pump causing fuel to flow from the fuel tank to the inlet port on the APU. After the turbine reaches full speed and can consume fuel without any additional assistance, the boost pump is turned off. This fuel continuously

combusts and causes the turbine to rotate, which transfers torque through the reduction drive assembly to the output shaft. The water brake dynamometer is attached to this shaft, and is controlled by a hose which is connected to a pressure regulator then to a manual valve outfitted with a pressure gauge. The pressure regulator prevents inconsistent water pressure from affecting the torque applied by the water brake. The flow rate of water is adjusted to create a consistent torque load on the output shaft of the APU.

To reduce noise effect, the APU test stand is located inside a building equipped with sound dampening foam. Exhaust gases flow out of the APU, through a ducting system outside of the building. The exhaust system contains a muffler to further reduce sound and the outlet side is directed upward to direct the noise away from the ground and populated areas.

2.3.2 APU Test Procedure

Before operation, the APU is checked to ensure that the equipment is fully functional and that there are no observable problems. A pre-test checklist is standard operating procedure before each run. The Electronic Sequence Unit (ESU) is used to start the APU and maintain its operation. The ESU automatically goes through the startup process, brings the APU to full operating speed, and maintains constant turbine speed. This process is controlled by the APU Tester, which can be seen on the left side of Figure 2.4.

The APU runs were performed uninterrupted for 45 minutes. Continuous vibration, oil temperature, exhaust temperature, RPM, fuel consumption, and torque readings were collected throughout the duration of each run. In addition to these readings, humidity, ambient temperature, and barometric pressure were recorded throughout each run. The

APU was shut down and allowed to cool to ambient temperature between runs. Seven runs were performed for Conventional, Batch A, and Batch B oils. All conventional oil testing was performed first; this prevented the possibility of contaminating the conventional oil with nano particles. The APU was flushed with conventional oil between Batch A and Batch B runs to remove any leftover nanodiamond particles. The dynamometer provided a consistent torque during the tests. The measurements taken during a 30 minute continuous torque portion of each test were compared.

Data is analyzed using RStudio and Microsoft Excel. The overall efficiency, oil temperature, and vibration data are compared between the oil types. The fuel flow rate is not directly compared, because slight inconsistencies in RPM and torque are present due to small variances in water pressure and the human error associated with manually adjusting the torque. To account for this, the overall efficiency of the APU is calculated and used for this study. This is performed using Equation 2.1. This relates the output power ($\dot{W}$) to the input power from the fuel ($\dot{E}_{in}$). Output power is calculated using Equation 2.2. RPM and torque were measured with the water brake dynamometer. The input power is determined from the mass flow rate of the fuel and the energy density of the fuel. The lower heating value is used for energy density, because energy is lost from the latent heat of vaporization. The input power calculation is shown in Equation 2.3

EQUATION 2.1 APU EFFICIENCY	$$Efficiency = \frac{\dot{W}}{\dot{E}_{in}}$$

EQUATION 2.2 OUTPUT POWER	$$\dot{W} = \frac{RPM \times Torque}{5252}$$

EQUATION 2.3 INPUT POWER	$$\dot{E}_{in} = Energy\ density_{fuel} \times \dot{m}_{fuel}$$

This approach is advantageous because it incorporates all of the losses in the system. If frictional losses increase or decrease, the efficiency will be affected. The efficiency comparison method also provides a way to normalize fuel flow data so that fuel consumption can be compared. Since efficiency represents the ratio of output power to input power, it can be used to study fuel flow for each oil type at specific horsepower values.

Vibration was measured with an accelerometer, which is mounted on the outside of the APU. The data was collected at 20 kHz. This resulted in about 15,000,000 data points per run. This data was analyzed by performing a Fast Fourier Transform (FFT) and by calculating the Root Mean Square value of each set of data. A FFT transforms the vibration data from a time domain to a frequency domain. It outputs vibration magnitudes with respect to the frequency at which they occur. This is useful because different rotating components vibrate at different resonance frequencies. The vibration of specific components can be compared between runs to show the benefits. The Root Mean Square value of each run was also found and then used to analyze differences between oil types. The RMS value is used to compare the overall vibration energy between oil types, while the FFT is used to compare vibration data occurring at individual frequencies. The RMS formula is shown in Equation 2.4. x represents the vibration data in a time domain. N

represents the number of values in the data. The square of the vibration data is averaged and then the square root is found.

<div align="center">

EQUATION 2.4 RMS EQUATION

$$RMS(x) = \sqrt{\frac{1}{N}\sum x^2}$$

</div>

Multiple studies suggest that ambient conditions can affect turbine efficiency[6,7]. This was accounted for by applying a correction factor to the fuel flow. Torque was held constant by the water brake and the APU maintains a constant rpm by adjusting fuel flow, so correction factors were not applied to the torque or rpm values. The fuel flow correction factor was originally developed by Warner and Auyer in 1945 and later analyzed by the National Advisory Committee for Aeronautics and the American Society of Mechanical Engineers. The equation for corrected fuel flow is shown in Equation 2.5. W_{fuel} represents the measured volumetric fuel flow. $W_{Corrected\ fuel}$ is the fuel flow after the correction is applied. δ is the ratio of measured barometric pressure to a standard sea level barometric pressure. θ is the ratio of measured ambient temperature to a standard temperature of 15°C. The corrected volumetric fuel flow is multiplied by the density of the fuel to determine the mass flow rate of the fuel[8].

<div align="center">

EQUATION 2.5 CORRECTED FUEL FLOW

$$W_{Corrected\ fuel} = \frac{W_{fuel}}{\delta\sqrt{\theta}}$$

</div>

Oil temperature was also corrected for effects caused by the difference in ambient temperature. Federal Aviation Regulations were used to account for these effects. The ambient temperature was subtracted from 100°F and then added to the oil temperature[9]. This can be seen in Equation 2.6.

Equation 2.6 Correction for Oil Temperature $$T_{oil\_corrected} = T_{oil} + (100°F - T_{ambient})$$

The average oil temperature throughout each run was determined, then a Tukey HSD test was performed to compare the runs for each oil type. All of the data is presented and discussed in Chapters 3 and 4.

2.4 Small Engine Test Stand

2.4.1 Description of Small Engine Test Stand
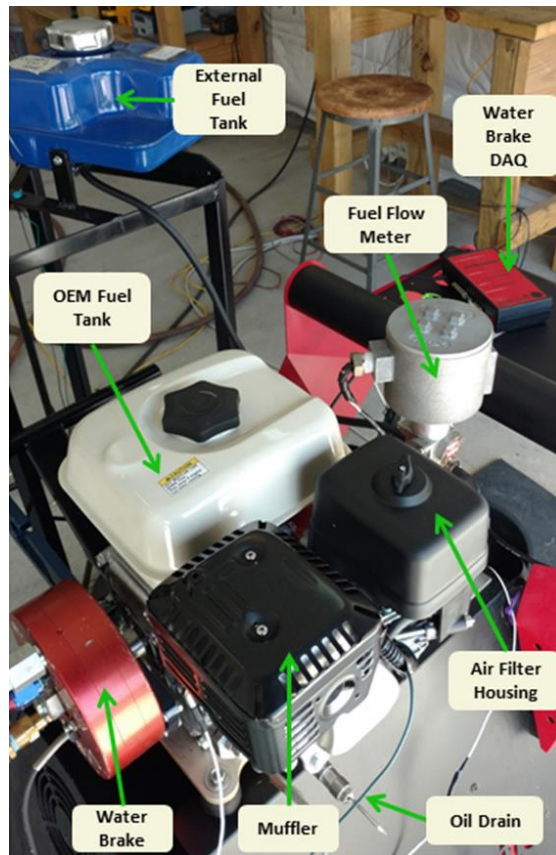
FIGURE 2.5 SMALL ENGINE TEST STAND

Figure 2.5 shows the Small Engine Test Stand. A 5.5 HP Honda GX200 4-stroke engine was used for this test. A fuel flow meter is mounted between the fuel tank and the engine to measure the fuel flow rate. The water brake dynamometer is attached to the output shaft so that a consistent torque load can be applied. RPM, torque, and ambient conditions are measured by the dynamometer. A DAQ utilizing LabView software is used for gathering oil temperature and fuel flow data.

2.4.2 Small Engine Test Procedure

A ten hour run was performed to break-in the engine. After this, four runs were performed for each type of oil. The engine was cooled after each sixty minute run until the oil temperature lowered to the ambient temperature. Five types of oil were tested. These include: Penzoil High Mileage 5W-30, Penzoil High Mileage 5W-30 with a nanodiamond additive, AeroShell 560, AeroShell 560 with nanodiamond particles (Batch A), and AeroShell 560 with graphene, zinc sulfide, and boron nitride particles (Batch B).

The Penzoil and AeroShell base oils were used to flush the engine between runs. This removed nanoparticles that were left in the engine and returned the engine to a baseline state. ANOVA and Tukey's HSD were used for analyzing data from the last 30 minutes of each run. This allowed time for the engine to reach steady state operating conditions. Equation 2.7 shows the correction factor used to account for variances in ambient barometric pressure and temperature. P is ambient barometric pressure in millibars and T is ambient temperature in °C. Equation 2.6 is used as the correction factor for oil temperature.

Equation 2.7 Correction Factor for Efficiency
$$cf = 1.176\left[\left(\frac{990}{P}\right)\left(\frac{T+273}{298}\right)^{\frac{1}{2}}\right] - 0.176$$

2.5 Procedures for Offline Analyses

2.5.1 Viscosity

Viscosity is measured using a Brookfield Engineering Co. LVDV II viscometer. This is a cone and plate type rotary viscometer. The torque meter used for this is a calibrated beryllium-copper spring which connects the rotating cone to the drive mechanism. A sample of the oil is placed between the cone and plate. The resistance to rotation, caused by the fluid, is then measured. This resistance creates a torque that is proportional to the shear stress in the fluid and this value is converted to dynamic viscosity in mPa·s from pre-calculated values in the software. The system is accurate to within ±1.0% and reproducibility is within ± 0.2% [10]. A Thermo NESLAB thermal bath was used to control the temperature of the sample and has a temperature accuracy of within 0.1°C. The Conventional, Batch A, and Batch B samples were tested at each ten degree increment ranging from 20°C to 90°C. Nine measurements were taken at each temperature.

2.5.2 Optical Microscopy

During the mixing process of the oils, clumps of particles were visibly noticeable in the original Batch B oil. To determine the size of these clumps, a KEYENCE VHX-5000 optical microscope with a lens capable of 5000x magnification was used. Batch A and Batch B were both examined and the size of the particle clumps was measured.

2.5.3 Transmission Electron Microscopy

A Hitachi H8000 TEM was used to measure the size of individual particles in the Batch B oil. This device has a resolution of 1.5 nm and a magnification of 2,000-800,000x. The sample had to be dried before it could be placed in the TEM. From there, the oil was diluted with acetone and placed on a hot plate with a magnetic stirring device. The acetone evaporated off, along with small amounts of oil. This was performed multiple times then the solution was placed on a wafer and allowed to dry before being placed in the machine. The types of the individual particles could not be identified, but their size could be measured.

CHAPTER 3: PRESENTATION OF RESULTS

3.1 TRDT Results

Temperature and vibration Condition Indicator (CI) data were analyzed and compared for the TRDT runs. CIs provide information about the condition of a mechanical component and are derived from accelerometer data by using signal processing methods. The CIs used for this study are Input FM4, Output FM4, Input DA1, and Output DA1.The fourth-order figure of merit (FM4) is used to find localized faults in gear teeth. These faults include chips, cracks, or spalling. FM4 is defined as the absolute kurtosis of the difference signal normalized by the square of variance of the difference signal[11]. Data Algorithm 1 (DA1) is useful for detecting an overall energy increase in the signal. This usually indicates a distributed gear fault, such as uniform wear of gear teeth. It is calculated by subtracting the RMS of the synchronous time average (STA) from the average of the STA[12]. The results for individual runs are shown in the following sections. The calculations used to compare Conventional Oil to Batch A.1 oil were performed in RStudio.

3.1.1 Conventional Oil Results

The average values along with the margins of error for each Conventional Oil run are shown in Table 3.1. It is shown that the percent error is below 2.3% for every run, which indicates the data is consistent throughout the iterations.

TABLE 3.1 TRDT DATA FOR CONVENTIONAL OIL

Conventional					
	Temp (° F)	**Input FM4**	**Output FM4**	**Input DA1**	**Output DA1**
Run 1	212.50 ± 1.53	3.23 ± 0.31	2.90 ± 0.11	7.31 ± 0.17	7.18 ± 0.18
Run 2	211.69 ± 2.35	3.23 ± 0.23	2.93 ± 0.15	7.37 ± 0.24	7.22 ± 0.20
Run 3	210.75 ± 3.30	3.36 ± 0.29	2.89 ± 0.18	7.31 ± 0.14	7.13 ± 0.13
Run 4	209.87 ± 3.16	3.58 ± 0.24	2.91 ± 0.13	6.78 ± 0.26	6.58 ± 0.24
Run 5	212.13 ± 2.45	3.33 ± 0.37	2.96 ± 0.16	6.70 ± 0.20	6.49 ± 0.20

3.1.2 Nano Oil Results

The average values along with the margins of error for each Batch A.1 run are shown in Table 3.2. The results for the temperature and all 4 CIs are provided. The percent error is below 1.6 % for every run.

TABLE 3.2 TRDT DATA FOR BATCH A.1

Batch A.1					
	Temp (° F)	**Input FM4**	**Output FM4**	**Input DA1**	**Output DA1**
Run 1	213.59 ± 1.29	3.46 ± 0.16	2.88 ± 0.17	6.99 ± 0.20	6.69 ± 0.13
Run 2	213.53 ± 2.10	3.56 ± 0.22	2.87 ± 0.11	7.20 ± 0.22	6.81 ± 0.20
Run 3	213.52 ± 1.77	2.99 ± 0.21	2.83 ± 0.13	7.25 ± 0.20	6.96 ± 0.18
Run 4	214.90 ± 2.06	3.45 ± 0.29	2.81 ± 0.17	7.50 ± 0.19	7.17 ± 0.15
Run 5	212.43 ± 2.61	3.21 ± 0.29	2.82 ± 0.17	7.32 ± 0.26	6.99 ± 0.21

3.1.3 TRDT Oil Comparison

The Temperature, Input FM4, Output FM4, Input DA1, and Output DA1 data, for every run of each type of oil was analyzed in RStudio. ANOVA and Tukey's honest significant difference (HSD) tests are used to analyze the data. ANOVA is used to determine the means of variables for multiple oil types. Tukey HSD is then used to apply a 95% confidence interval and to compare the values calculated by the ANOVA test.

TABLE 3.3 TRDT OIL DATA COMPARISON

	Temp [C]	InputFM4	OutputFM4	Input DA1	Output DA1
Change from Conv to Batch A.1	1.22 ± 0.38	-0.01 ± 0.09	-0.08 ± 0.04	0.16 ± 0.09	0.00 ± 0.09
p-value	1.57E-09	0.749	0.000361	0.0004508	0.92001

The results from the Tukey's HSD test are shown in Table 3.3. The difference in means of the data is statistically significant for Temperature, Output FM4, and Input DA1. There is not a significant difference for Input FM4 and Output DA1, so those CIs were not affected by the oil type. The Temperature and Input DA1 CIs were both higher with the Batch A.1 oil. Output FM4 was slightly lower for Batch A.1.

After reviewing these results, it was determined that the concentration of nanodiamond particles was too low in Batch A.1. A new oil, Batch A.2, was developed for further testing. There were multiple concentrations of Batch B, so the No Load test stand was used to compare these concentrations, along with the Batch A.2 oil, to determine the optimal oils for APU testing. The lower cost of No Load testing results in a more efficient testing method to compare these oils.

3.2 No Load Test Results

Temperature data from the last 20 minutes of each run was analyzed in RStudio. ANOVA and Tukey's HSD tests were used to analyze the data. Table 3.4 shows the results from the No Load testing. Conventional oil was tested first. The difference in average temperature between conventional oil and each nano oil, at each location, is shown in this table. A positive value indicates that the temperature rose by that amount, while a negative value indicates that the temperature decreased by that amount.

TABLE 3.4 NO LOAD TEMPERATURE DIFFERENCES (°F)

	IDB	IRB	ORB	ODB
Batch B.1	-8.06	-10.2	-9.39	-13.46
Batch A.2	-2.45	-0.95	-1.08	-1.19
Batch B.2	-2.78	-8.65	-10.93	-11.89
Batch B.3	5.45	-7.84	-15.53	-13.07

From this table, it is evident that all of the nano oils reduced the temperature in the gearbox for at least three of the four thermocouples. Batch A.2 had the smallest average temperature reduction. Batch B.1 provided the best temperature reduction across all 4 thermocouples. Batch B.2 had the second smallest reduction, but still performed well on the output side of the gearbox. Batch B.3 provided the largest temperature reduction in the output side of the gearbox, but increased the temperature near the Input Duplex Bearing.

As a result of this testing, Batch B.1 was selected for testing in the APU, along with Batch A.2. For the rest of this document Batch B.1 will be referred to simply as Batch B and Batch A.2 will be referred to as Batch A.

3.3 APU Test Results

3.3.1 Conventional Oil

Efficiency:

Calculations were first performed in Excel to determine the consistency of each run. This ensures that there is not a large amount of variance within each set of data. Table 3.5 contains results from data associated with each run of conventional oil. The mean values for each variable are provided. A t-test is performed to determine the percent error

22

in the data for a 95% confidence interval. The equation for percent error in a data set is shown in Equation 3.1. The variance in the data is multiplied by the $t_{critical}$ value and divided by the square root of the degree of freedom. Torque is the controlled variable. A pressure regulator, along with manual adjustment of a valve, results in a very consistent torque load throughout each run. This is evident from the small percent error in each run's set of data. Fuel flow is the dependent variable. Equation 2.1 is used to find efficiency from horsepower and flow rate. The data analyzed from the final 30 minutes of each run consisted of approximately 1,800 data points for fuel flow and efficiency. Torque and RPM were sampled more frequently and consisted of about 18,000 data points.

EQUATION 3.1

$$Percent\ Error = \frac{Variance \times t_{critical}}{\sqrt{degree\ of\ freedom}}$$

TABLE 3.5 CONVENTIONAL OIL APU DATA

Conventional					
	Fuel Flow (mL/s)	**HP**	**RPM**	**Torque(ft-lb)**	**Efficiency**
Run 1	13.11	34.00	12022.32	14.86	5.48
Run 2	13.19	33.81	12024.19	14.77	5.42
Run 3	12.90	34.04	12009.54	14.89	5.58
Run 4	12.73	33.58	11998.14	14.70	5.57
Run 5	12.72	33.81	11987.68	14.81	5.61
Run 6	12.98	33.78	12018.55	14.76	5.50
Run 7	12.86	33.86	12006.95	14.81	5.56

Table 3.6 shows the average values across all seven runs. The standard deviation is not shown since it is less than the error associated with the measuring devices, because of the large number of data points collected during each run. 14.80 ft-lb of torque was applied and the output shaft spun at 12009.62 RPM. This results in 33.84 hp of output power. The

corrected fuel rate is 12.93 mL/s. The APU was 5.53% efficient during the seven runs with

conventional oil.

TABLE 3.6 CONVENTIONAL OIL DATA FOR 7 RUNS

Conventional Average					
	Fuel Flow(mL/s)	Hp (Hp)	Brake (RPM)	Torque (ft-lb)	Efficiency (%)
Mean	12.93	33.84	12009.62	14.80	5.53
Standard Deviation	0.18	0.15	13.38	0.06	0.07
Variance	0.03	0.02	178.91	0.00	0.00
n	7.00	7.00	7.00	7.00	7.00
df	6.00	6.00	6.00	6.00	6.00
t statistic (df) (95%)	2.37	2.37	2.37	2.37	2.37
Margin of Error	0.03	0.02	172.74	0.00	0.00
% Error	0.23%	0.07%	1.44%	0.03%	0.08%

Oil Temperature:

The oil temperature was analyzed from the 15 to 45 minute portion of each run.

The correction factor was applied by using Equation 2.6. This correction factor was

designed to be used for temperature in Fahrenheit. The data was then converted to Celsius

before the Tukey HSD test was performed. The average oil temperature for each run can

be seen in Table 3.7. The averages for each run are shown with and without the correction

for ambient temperature effects.

TABLE 3.7 CONVENTIONAL OIL TEMPERATURES

	Oil Temp [°F]	Oil Temp [°C]	Corrected Temp [°F]	Corrected Temp [°C]
Conventional Oil				
Run 1	170.45	76.92	211.18	99.54
Run 2	169.14	76.19	211.76	99.87
Run 3	182.41	83.56	214.07	101.15
Run 4	187.90	86.61	211.94	99.97
Run 5	189.51	87.50	210.21	99.01
Run 6	175.80	79.89	211.85	99.92
Run 7	180.79	82.66	210.25	99.03
Mean	179.43 ± 8.00	81.90 ± 4.44	211.61 ± 1.31	99.78 ± 0.73

Equation 2.6 corrects the oil temperature to represent the results that would be expected for an ambient temperature of 100°F (37.78°C). From this table, it is evident that the correction factor greatly reduced the percent error in the data between the seven runs.

Vibration:

TABLE 3.8 VIBRATION DATA FOR CONVENTIONAL OIL

	Peak Magnitude	Peak Frequency Location (Hz)	RMS
Conventional Oil Vibration Data			
Run 1	2.23	6426.90	21.95
Run 2	2.54	6426.10	23.58
Run 3	3.05	6417.00	28.85
Run 4	2.86	6413.20	31.76
Run 5	3.27	6404.80	31.85
Run 6	2.48	6420.70	26.31
Run 7	1.25	6420.20	16.98
Mean	2.53 ± 0.66	6418.41 ± 7.68	25.90 ± 5.46

Table 3.8 shows the vibration data for the runs performed with conventional oil. The average peak magnitude occurs at a frequency of 6,418.41 Hz. The variation in this is caused by the rotational speed of the drive shaft during each run. The average peak magnitude is 2.53 g and the average RMS is 25.90 g.

3.3.2 Batch A

Efficiency:

Table 3.9 shows the results for each run of Batch A oil. Each run has approximately the same number of data points as the conventional runs. The large number of data points causes the percent error to be extremely small.

TABLE 3.9 BATCH A OIL DATA

Batch A				
	Fuel Flow (mL/s)	**HP**	**RPM**	**Torque(ft-lb)**	**Efficiency**
Run 1	12.80	33.89	11997.60	14.84	5.59
Run 2	12.97	33.70	12017.12	14.73	5.49
Run 3	12.78	33.87	12004.91	14.82	5.60
Run 4	12.58	33.87	11985.65	14.84	5.69
Run 5	12.73	33.60	11994.50	14.71	5.58
Run 6	12.75	33.67	12008.88	14.72	5.58
Run 7	12.66	33.71	11991.58	14.76	5.62

Table 3.10 shows the average fuel flow, HP, RPM, torque, and efficiency values for all seven Batch A runs. 14.77 ft-lb of torque was applied and the output shaft spun at 12000.03 RPM. The APU burned fuel at a corrected rate of 12.75 mL/s. The efficiency is 5.59%.

TABLE 3.10 BATCH A OIL AVERAGE FOR 7 RUNS

Batch A Average					
	Fuel Flow(mL/s)	**Hp (Hp)**	**Brake (RPM)**	**Torque (ft-lb)**	**Efficiency (%)**
Mean	12.75	33.76	12000.03	14.77	5.59
Standard Deviation	0.12	0.12	10.87	0.06	0.06
Variance	0.01	0.01	118.11	0.00	0.00
n	7.00	7.00	7.00	7.00	7.00
df	6.00	6.00	6.00	6.00	6.00
t statistic (df) (95%)	2.37	2.37	2.37	2.37	2.37
Margin of Error	0.01	0.01	114.04	0.00	0.00
% Error	0.11%	0.04%	0.95%	0.02%	0.06%

Oil Temperature:

Table 3.11 shows the average oil temperature for each run. The averages are shown with and without the correction for ambient temperature effects.

TABLE 3.11 BATCH A OIL TEMPERATURES

Batch A Oil				
	Oil Temp(°F)	Oil Temp(°C)	Corrected Temp(°F)	Corrected Temp(°C)
Run 1	184.68	84.82	211.69	99.83
Run 2	171.91	77.73	209.97	98.87
Run 3	181.22	82.90	210.95	99.42
Run 4	185.89	85.49	205.99	96.66
Run 5	183.40	84.11	205.15	96.19
Run 6	177.54	80.86	211.35	99.64
Run 7	182.17	83.43	208.51	98.06
Mean	180.97 ± 4.82	82.77 ± 2.68	209.09 ± 2.63	98.38 ± 1.46

As was the case for conventional oil, the correction for ambient temperature effects caused the percent error in the data to be substantially reduced. This data is compared to the data for conventional oil in section 3.3.1.

Vibration:

TABLE 3.12 VIBRATION DATA FOR BATCH A OIL

Batch A Vibration Data			
	Peak Magnitude	**Peak Frequency Location (Hz)**	**RMS**
Run 1	2.30	6411.50	23.80
Run 2	2.42	6423.80	26.63
Run 3	2.10	6417.20	22.05
Run 4	1.26	6405.30	17.05
Run 5	0.71	6411.40	15.52
Run 6	1.00	6417.90	17.23
Run 7	1.75	6408.70	19.25
Mean	1.65 ± 0.67	6413.69 ± 6.29	20.22 ± 4.07

Table 3.12 shows the vibration data for Batch A oil. The average peak magnitude occurs at a frequency of 6,413.69 Hz. The average peak magnitude is 1.65 g and the average RMS is 20.22 g.

3.3.3 Batch B

Efficiency:

Table 3.13 provides data for each of the Batch B runs. The percent error in the data is less than two hundredths of a percent for every variable.

TABLE 3.13 BATCH B OIL DATA FOR 7 RUNS

	Fuel Flow (mL/s)	HP	RPM	Torque(ft-lb)	Efficiency
	Batch B				
Run 1	12.70	33.76	12012.45	14.76	5.61
Run 2	12.55	33.66	12006.26	14.72	5.67
Run 3	12.39	34.09	11968.97	14.96	5.81
Run 4	12.73	33.84	12010.53	14.80	5.62
Run 5	12.48	33.63	11989.59	14.73	5.69
Run 6	12.29	33.68	11970.98	14.78	5.79
Run 7	12.35	33.21	11971.35	14.57	5.68

The average data for each variable is provided in Table 3.14. The efficiency is 5.70%, the fuel flow is 12.50 mL/s, the RPM was 11,990.02, the torque is 14.76 ft-lbs, and the output power was 33.70 HP.

TABLE 3.14 BATCH B OIL AVERAGE FOR 7 RUNS

	Fuel Flow(mL/s)	Hp (Hp)	Brake (RPM)	Torque (ft-lb)	Efficiency (%)
	Batch B Average				
Mean	12.50	33.70	11990.02	14.76	5.70
Standard Deviation	0.17	0.27	19.76	0.12	0.08
Variance	0.03	0.07	390.32	0.01	0.01
n	7.00	7.00	7.00	7.00	7.00
df	6.00	6.00	6.00	6.00	6.00
t statistic (df) (95%)	2.37	2.37	2.37	2.37	2.37
Margin of Error	0.03	0.07	376.86	0.01	0.01
% Error	0.23%	0.20%	3.14%	0.09%	0.10%

Oil Temperature:

The oil temperature data for Batch B is shown in Table 3.15. The temperatures, with and without the ambient temperature correction, are provided. Again, the percent error is reduced. The average temperature is noticeably higher than it is for Conventional and Batch A testing.

TABLE 3.15 BATCH B OIL TEMPERATURES

Batch B Oil				
	Oil Temp(°F)	Oil Temp(°C)	Corrected Temp(°F)	Corrected Temp(°C)
Run 1	203.63	95.35	227.68	108.71
Run 2	204.68	95.93	225.27	107.37
Run 3	211.83	99.90	219.01	103.89
Run 4	199.90	93.28	227.87	108.82
Run 5	208.14	97.86	224.06	106.70
Run 6	217.68	103.16	221.31	105.17
Run 7	216.99	102.77	223.35	106.31
Mean	208.98 ± 6.81	98.32 ± 3.78	224.08 ± 3.23	106.71 ± 1.80

Vibration:

TABLE 3.16 VIBRATION DATA FOR BATCH B OIL

Batch B Vibration Data			
	Peak Magnitude	Peak Frequency Location (Hz)	RMS
Run 1	1.62	6422.80	18.78
Run 2	0.87	6417.50	15.49
Run 3	2.30	6396.80	24.03
Run 4	0.90	6416.70	15.79
Run 5	1.33	6405.20	18.62
Run 6	1.35	6391.20	18.93
Run 7	1.43	6396.80	21.88
Mean	1.40 ± 0.48	6406.71 ± 12.34	19.07 ± 3.06

The vibration data for Batch B is provided in Table 3.16. The average peak magnitude is 1.40 g and occurs at 6,406.71 Hz. The average RMS is 19.07 g. These values show that the APU had lower vibration using Batch B than with Batch A or conventional oil.

3.3.4 APU Oil Comparison

The efficiency, oil temperature, and vibration data were compared for all three oils. This was performed by running an ANOVA test and a Tukey HSD with RStudio. This test outputs the difference in each variable, between each type of oil. A 95% confidence interval was chosen.

Efficiency:

Batch A and Batch B are each compared to the conventional oil. The results suggest that both improve overall APU efficiency. The p-value is calculated as part of the Tukey HSD test. It is calculated to determine if values are significantly different and can range from zero to one. A small p-value, typically less than 0.05, means that the calculated values are different. The p-value is less than 2×10^{-16} for all of these calculations. This provides very good evidence that the data is statistically different. This test was performed for a 95% confidence interval. It can be seen from the boxplot in Figure 3.1 that Batch B has the highest efficiency. Figure 3.2 provides another visual representation of the data with the efficiency graphed for each run. From the Tukey HSD test, the efficiency for Batch A oil is 0.05% higher than conventional and the efficiency for Batch B is 0.16% higher than that

of Conventional oil. The average values for fuel flow, torque, RPM, and efficiency are shown in Table 3.17.

TABLE 3.17 EFFICIENCY AND FUEL FLOW RESULTS

Oil Type	Average Corrected Fuel Flow (mL/s)	Average Output Torque (ft-lb)	Average RPM	Average Efficiency(%)
Conventional	12.93	14.80	12009.62	5.54
Batch A	12.75	14.77	12000.03	5.59
Batch B	12.50	14.76	11990.02	5.70
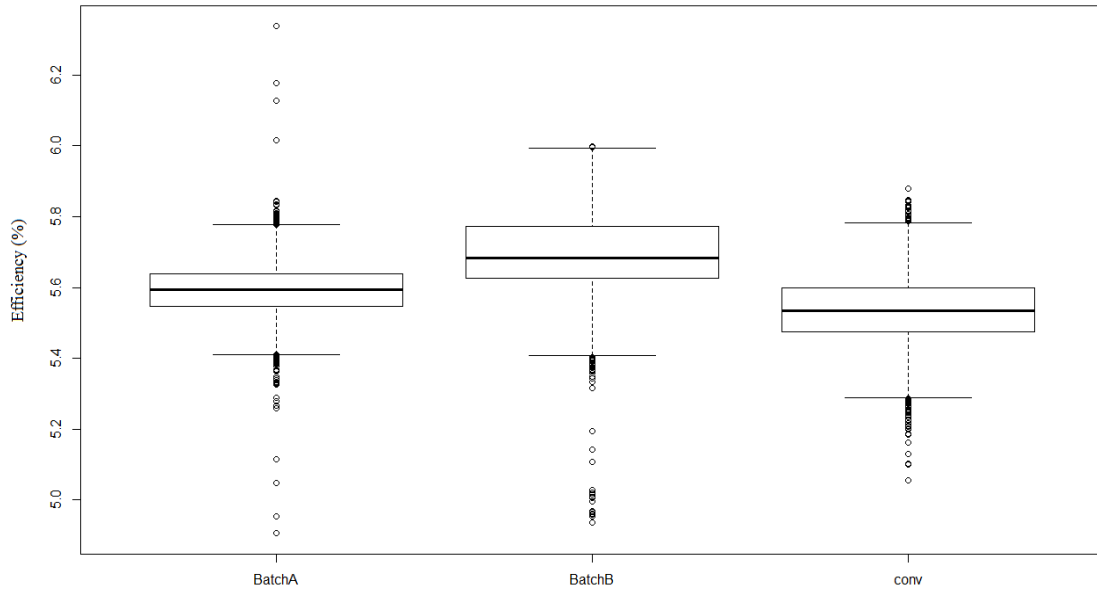
FIGURE 3.1 BOXPLOTS OF OIL EFFICIENCY FOR EACH OIL TYPE
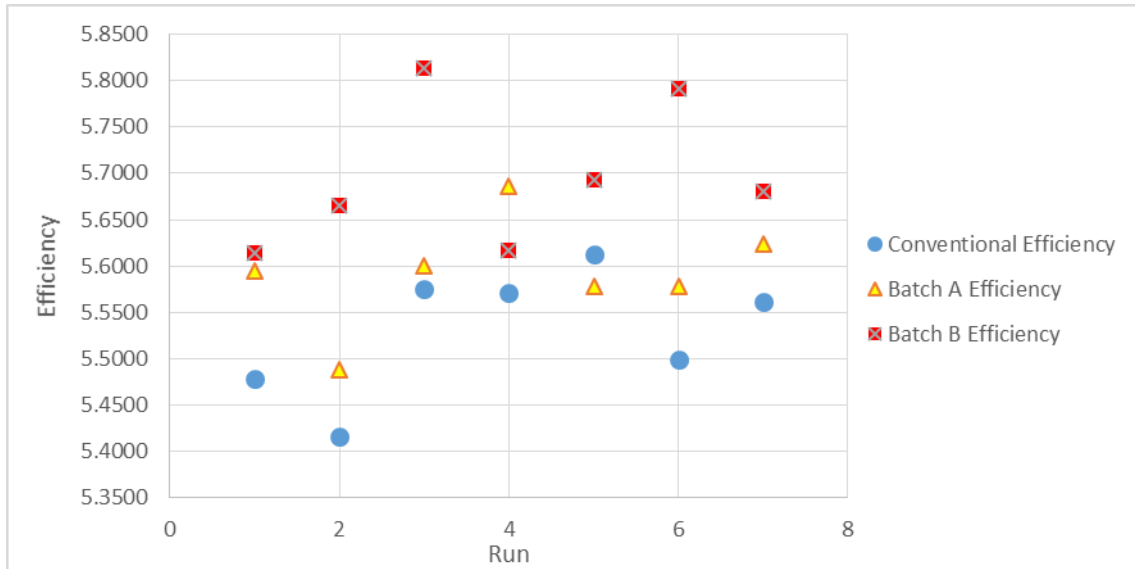
FIGURE 3.2 EFFICIENCY GRAPH FOR EACH RUN

Temperature:

Based on the RStudio results with a 95% confidence interval, Batch A reduced the average oil temperature by 1.40 °C. However, the p-value for that comparison was 0.1755, so the difference in those data sets are not statistically significant. Batch B increased the temperature by 6.93 °C. The p-value for this comparison was $1\text{x}10^{-7}$. This shows that there is a definite statistical difference between the mean oil temperature of the conventional oil and Batch B oil.

TABLE 3.18 OIL TEMPERATURE RESULTS

	Oil Temp [°F]	Oil Temp [°C]	Corrected Temp [°F]	Corrected Temp [°C]
Conventional	179.43 ± 8.00	81.90 ± 4.44	211.61 ± 1.31	99.78 ± 0.73
Batch A	180.97 ± 4.82	82.77 ± 2.68	209.09 ± 2.63	98.38 ± 1.46
Batch B	208.98 ± 6.81	98.32 ± 3.78	224.08 ± 3.23	106.71 ± 1.80
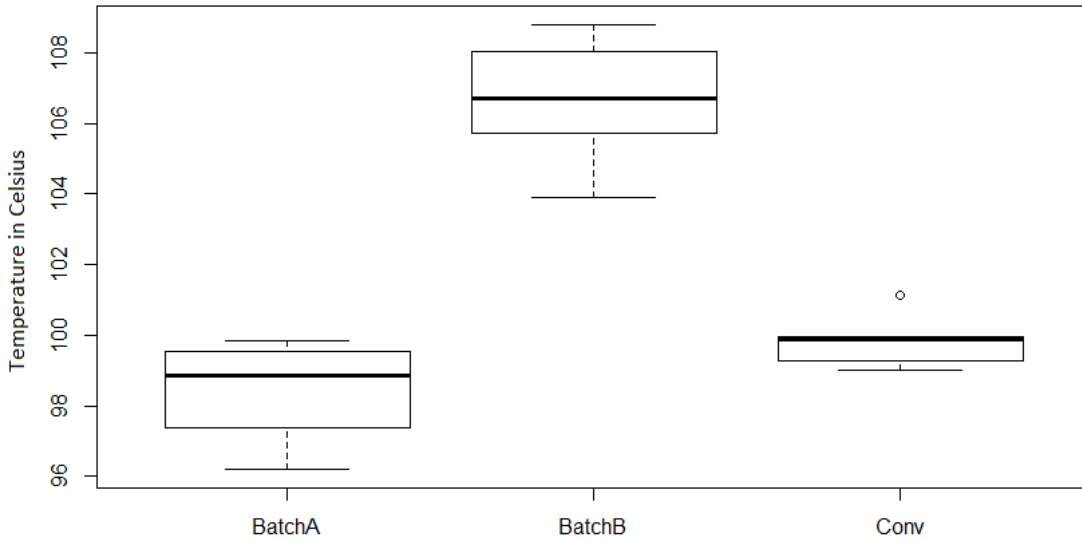
FIGURE 3.3 BOX PLOT OF OIL TEMPERATURES

Figure 3.3 is a box plot of the oil temperatures. From the figure, it is evident that the Batch B oil operated at a much higher temperature than the other two oils. An increase in temperature can be a result of increased friction or from increased heat transfer from a higher temperature at another location, such as the combustor.

Vibration:

The vibration data for each type of nano oil is compared to the conventional oil using RStudio. ANOVA and Tukey HSD tests were used to analyze the data.

TABLE 3.19 BATCH A AND BATCH B VS CONVENTIONAL RESULTS

Vibration Data for Nano Oils Compared to Conventional Oil				
Oil Comparison	Peak Magnitude (g)	p-value for Magnitude	RMS (g)	p-value for RMS
Batch A vs Conventional	-0.88	0.04	-5.68	0.06
Batch B vs Conventional	-1.12	0.01	-6.82	0.02

Table 3.19 shows the vibration results. The values represent the reduction in vibration when using each nano oil instead of conventional oil. The p values are also shown for each calculation. The p-value for the RMS comparison between Batch A and conventional is very close to 0.05, so the statistical significance of that RMS value is questionable. The other values are well below 0.05, so they are statistically significant. Both oils show a reduction in peak vibrations and RMS, but Batch B shows a larger decrease in both types of vibration. This is important because energy is converted to create vibration and can result in a decrease in efficiency. Excessive vibration can also accelerate wear and component failures.

3.4 Small Engine Results

3.4.1 Efficiency

Table 3.20 shows the efficiency results for each run for all five types of oil along with the average efficiency for each type.

TABLE 3.20 SMALL ENGINE EFFICIENCY RESULTS

Oil Type	Average Efficiency for Individual Runs	Average Efficiency of Oil Type
Pennzoil 1	20.95%	
Pennzoil 2	22.50%	
Pennzoil 3	21.17%	21.29%
Pennzoil 4	20.57%	
Pennzoil w/ ND Additive 1	19.74%	
Pennzoil w/ ND Additive 2	20.75%	
Pennzoil w/ ND Additive 3	21.85%	20.88%
Pennzoil w/ ND Additive 4	21.18%	
Conventional (AeroShell 560) 1	21.80%	
Conventional (AeroShell 560) 2	21.95%	
Conventional (AeroShell 560) 3	22.01%	21.83%
Conventional (AeroShell 560) 4	21.58%	
Batch A.2 1	21.88%	
Batch A.2 2	22.09%	
Batch A.2 3	21.08%	21.58%
Batch A.2 4	21.26%	
Batch B.1 1	21.90%	
Batch B.1 2	22.56%	
Batch B.1 3	22.55%	22.43%
Batch B.1 4	22.71%	

The efficiency was higher for conventional turbine oil than Pennzoil. This is interesting, because Pennzoil is recommended for use in the engine. The use of nanodiamond particles reduced the efficiency of both oils while the use of Batch B.1 resulted in increased efficiency. Table 3.21 shows the results calculated with a Tukey HSD test. The efficiency of Batch B.1 was 0.6% higher than that of the conventional turbine oil.

TABLE 3.21 COMPARISON OF SMALL ENGINE EFFICIENCY RESULTS

Oil Type	p-Value	Difference (95% conf.)
Pennzoil	< 2E-16	███████████
Pennzoil w/ ND Additive		-0.44%
Conventional (AeroShell 560)	< 2E-16	███████████
Batch A.2		-0.26%
Batch B.1		0.60%

Temperature:

Table 3.22 shows the temperature results for each run for all five types of oil along with the average efficiency for each type.

TABLE 3.22 SMALL ENGINE TEMPERATURE RESULTS

Oil Type	Average Temperature for Individual Runs (°C)	Average Temperature for Oil Type (°C)
Pennzoil 1	105.81	
Pennzoil 2	104.14	106.81
Pennzoil 3	107.85	
Pennzoil 4	109.46	
Pennzoil w/ ND Additive 1	112.34	
Pennzoil w/ ND Additive 2	105.44	104.73
Pennzoil w/ ND Additive 3	98.19	
Pennzoil w/ ND Additive 4	102.94	
Conventional (AeroShell 560) 1	104.28	
Conventional (AeroShell 560) 2	104.02	105.28
Conventional (AeroShell 560) 3	105.32	
Conventional (AeroShell 560) 4	107.49	
Batch A.2 1	104.76	
Batch A.2 2	104.86	103.52
Batch A.2 3	105.51	
Batch A.2 4	98.98	
Batch B.1 1	103.93	
Batch B.1 2	102.24	103.64
Batch B.1 3	102.33	
Batch B.1 4	106.08	

The oil temperature was also lower for AeroShell oil than for Pennzoil. The addition of nanodiamonds resulted in lower oil temperatures for both oil types. The conventional oil containing graphene, zinc sulfide, and boron nitride particles also operated at a lower oil temperature than the conventional oil. The data comparison from the Tukey HSD results can be seen in Table 3.23.

TABLE 3.23 COMPARISON OF SMALL ENGINE TEMPERATURE RESULTS

Oil Type	p-Value	Difference(°C) (95% conf.)
Pennzoil	< 2E-16	██████████
Pennzoil w/ ND Additive		-1.67
Conventional (AeroShell 560)	< 2E-16	██████████
Batch A.2		-1.88
Batch B.1		-1.63

Vibration:

Table 3.24 shows the vibration results for each run of all five types of oil in addition to the average efficiency for each type.

TABLE 3.24 SMALL ENGINE VIBRATION RESULTS

Oil Type	RMS (*g*)	Avg RMS (g)
Pennzoil 1	1.870	
Pennzoil 2	1.888	1.879
Pennzoil 3	1.855	
Pennzoil 4	1.902	
Pennzoil w/ND additive 1	1.826	
Pennzoil w/ND additive 2	1.874	1.886
Pennzoil w/ND additive 3	1.919	
Pennzoil w/ND additive 4	1.923	
Conventional (AeroShell 560) 1	1.953	
Conventional (AeroShell 560) 2	1.957	1.957
Conventional (AeroShell 560) 3	2.000	
Conventional (AeroShell 560) 4	1.917	
Batch A.2 1	1.961	
Batch A.2 2	2.051	1.971
Batch A.2 3	1.933	
Batch A.2 4	1.940	
Batch B.1 1	1.672	
Batch B.1 2	1.647	1.656
Batch B.1 3	1.654	
Batch B.1 4	1.653	

Unlike the efficiency and temperature results, the conventional oil resulted in higher vibration values than Pennzoil. The nanodiamond additives increased overall vibration when used in both types of oil, but not significantly. The Batch B.1 runs had the lowest RMS values and using this oil instead of conventional oil resulted in a 15.4% reduction in RMS. The vibration comparisons from the Tukey HSD test are shown in Table 3.25. Based on the p-values, the addition of nanodiamond particles did not result in a statistically significant change in RMS values. The p-value for Batch B.1 is much lower than 0.05, so 15.4% reduction in vibration is statistically significant.

TABLE 3.25 COMPARISON OF SMALL ENGINE VIBRATION DATA

Oil Type	p-Value	Difference *(g)* (95% conf.)
Pennzoil		██████████████
Pennzoil w/ ND Additive	0.793	0.007
Conventional (AeroShell 560)		██████████████
Batch A.2	0.846	0.015
Batch B.1	1E-07	-0.300

3.5 Results From Offline Analyses

3.5.1 Viscosity

The viscosity of each oil was measured from 20° to 90°C. The samples were measured at various shear stresses and were determined to be Newtonian fluids, which means that the shear stress varies linearly with shear rate. These results show the viscosity change with temperature for Conventional, Batch A, and Batch B oils.

Table 3.26 Dynamic Viscosities of Oils at Various Temperatures

Temperature (°C)	Conventional (Pa*s)	Batch A (Pa*s)	Batch B (Pa*s)
20	0.0668	0.0666	0.0672
30	0.0395	0.0408	0.0411
40	0.0262	0.0266	0.0277
50	0.0181	0.0188	0.0198
60	0.0132	0.0138	0.0148
70	0.0087	0.0106	0.0107
80	0.0076	0.0083	0.0086
90	0.0061	0.0067	0.0072
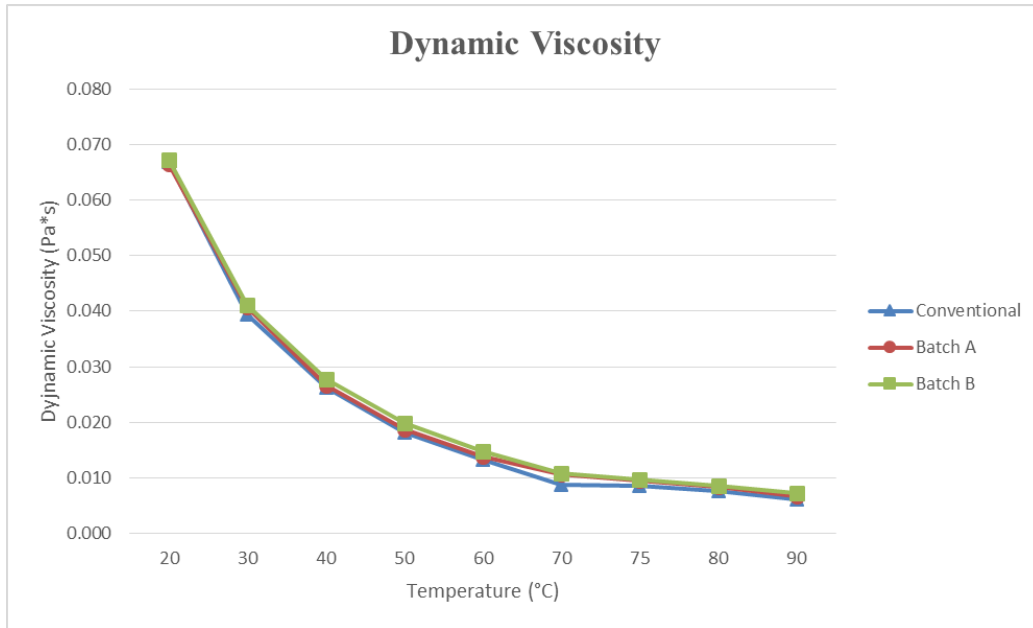
FIGURE 3.4 GRAPH OF OIL VISCOSITIES

Table 3.26 and Figure 3.4 show the dynamic viscosities of the three types of oil. Batch A has a higher viscosity than Conventional oil and Batch B has the highest viscosity at every temperature. It is important for an oil to maintain an acceptable viscosity at higher temperatures if it is designed for use in a jet engine. The oil temperature in the APU was between 85°C and 105°C for most of the runs. At 90°C, the viscosity of Batch B was 17.97% higher than the viscosity of the Conventional oil. This would cause a reduction in surface to surface contact, but also increase the drag force associated with spinning a bearing in oil. It is important to maximize the reduction in surface contact while keeping the drag force as low as possible.

40

3.5.2 Optical Microscopy

The optical microscope showed that there were large particles present in the initial Batch B oil. Some of these particles were over 200µm. This can be seen in Figure 3.5.
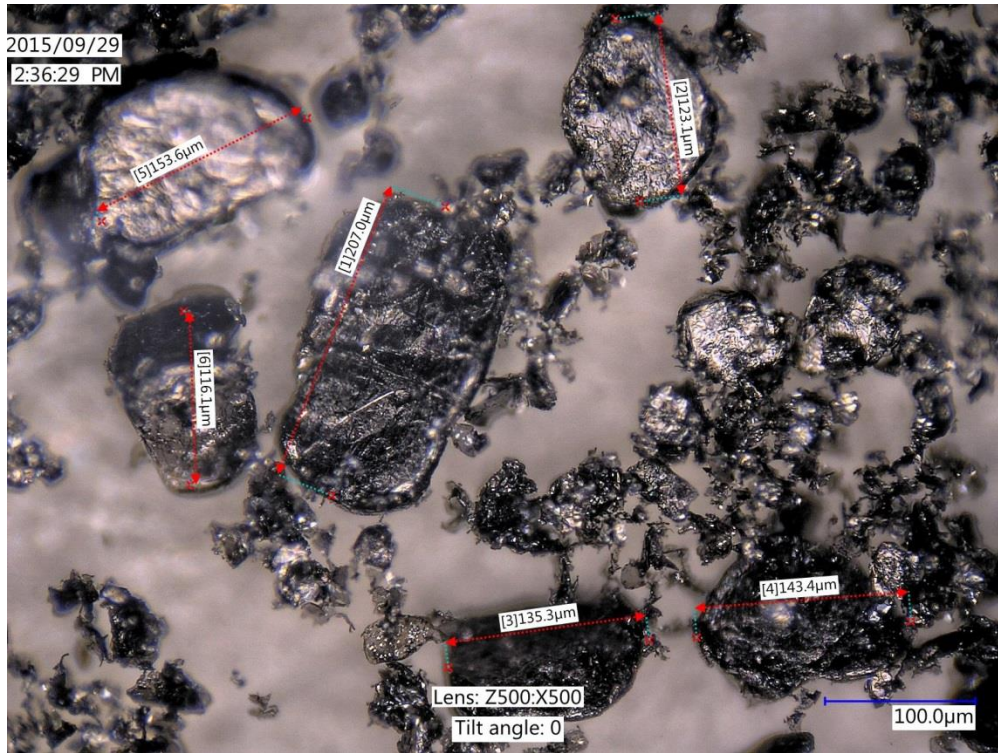
FIGURE 3.5 IMAGE OF LARGE PARTICLES IN THE INITIAL BATCH B NANO OIL

Because these particles are so much larger than the pores in the APU oil filter, a second Batch B oil was created to remove these large particles. The initial Batch B oil was passed through a filter by NanoPro MT. While the particle size was reduced, Figure 3.6 shows that they were still in the 20 to 40µm range. The APU has a 10µm oil filter, so these particles could still clog the filter.
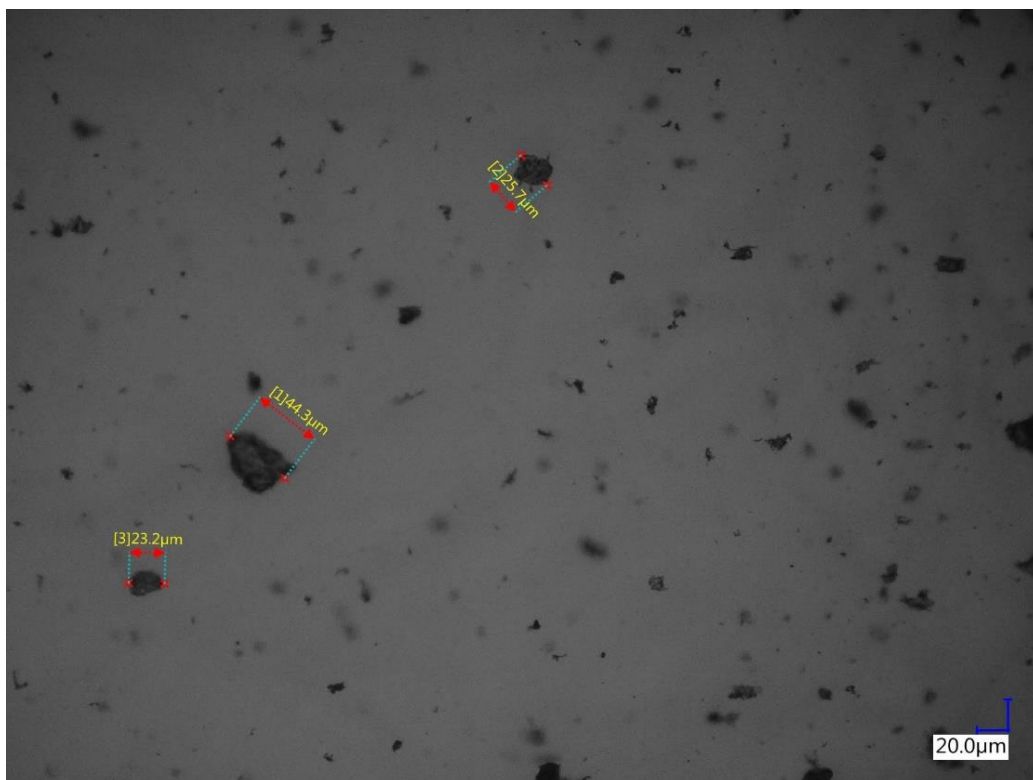
FIGURE 3.6 IMAGE OF BATCH B NANO OIL

The nanodiamond particle clumps are much smaller than the ones present in Batch B. Figure 3.7 shows the Batch A oil when viewed through an optical microscope. Most of the clumped particles are in the 6 to 12µm range.
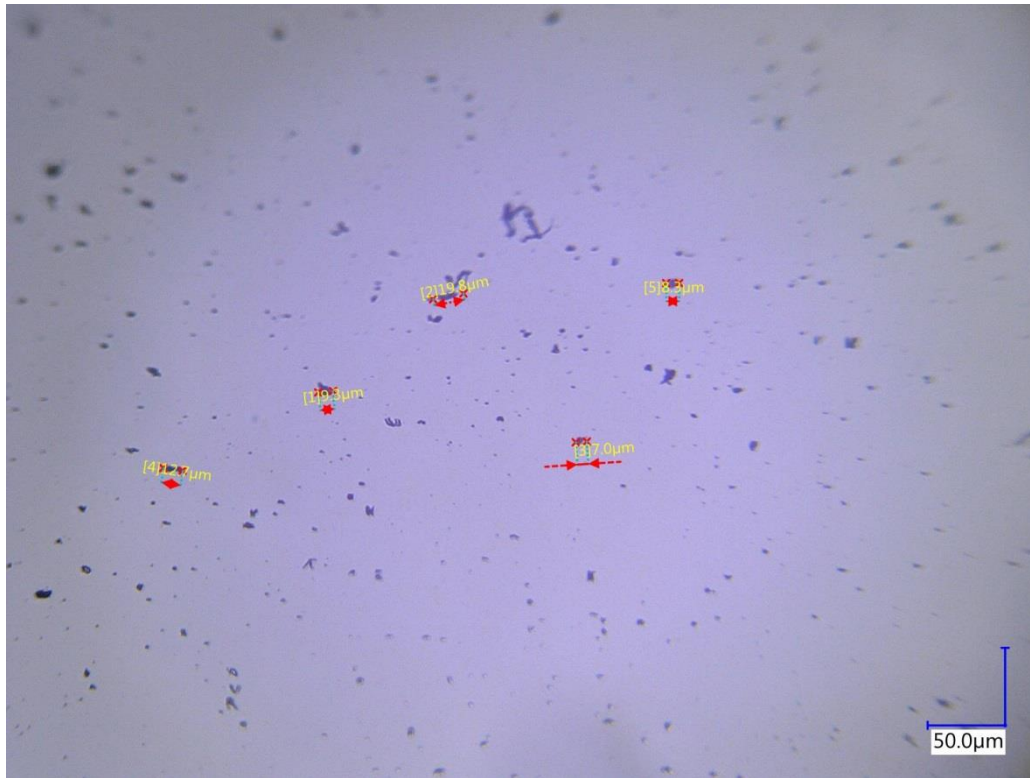
FIGURE 3.7 IMAGE OF NANO OIL BATCH A

3.5.3 Transmission Electron Microscopy

The Batch B particles were dried and observed with a transmission electron microscope (TEM). The optical microscope could view the large clumps, but not the individual particles. Figure 3.8 is an image taken with the TEM. Some of the oil could not be removed. This caused the large clump of particles in the center of the image. A few individual nano particles are circled in red. Based on the scale, these particles are very close to 4nm. This suggests that the large particles observed with the optical microscope are clumps of these nano particles.

43
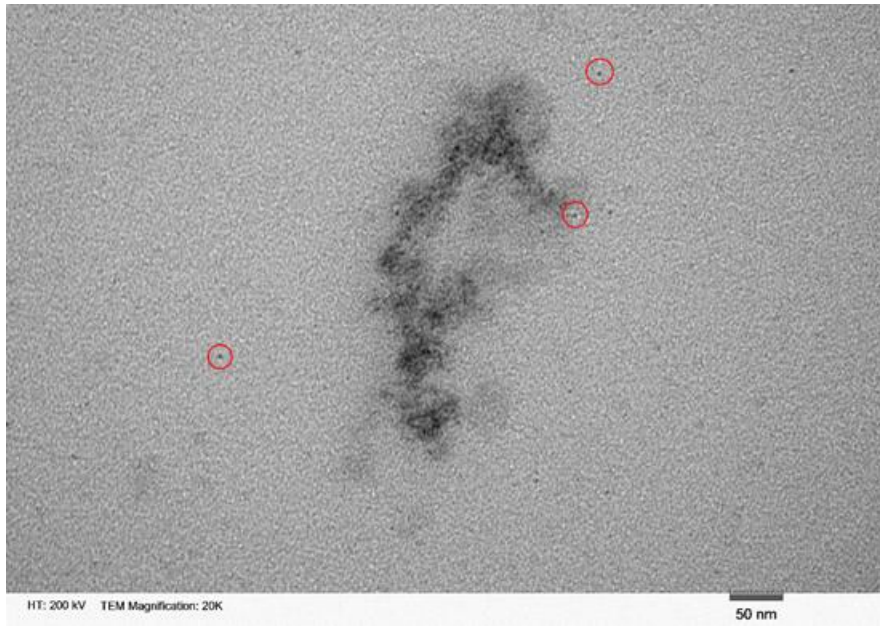
FIGURE 3.8 TEM IMAGE OF NANO PARTICLES

CHAPTER 4: DISCUSSION OF RESULTS

The results presented in Chapter 3 are discussed in this chapter. The knowledge gained from offline analyses is used during the discussion of results from the test stands. These results are supplemented with data and findings from previous studies.

4.1 Tail Rotor Drivetrain

The primary determination from the TRDT test was that Batch A needed to be more concentrated. Two vibration CIs did not have a statistically significant change, while the other two showed very small changes between the conventional and Batch A runs. Since the changes were so miniscule, it was determined that more testing needed to be performed to determine the necessary concentration of nano particles. Since multiple tests needed to be performed, the No Load Test Stand was used. The No Load is much cheaper to operate and requires less maintenance time between runs, so it is the optimal choice for initial testing of multiple oils.

4.2 No Load Test Stand

The reason that Batch B provided a greater cooling effect than Batch A is most likely because of the higher concentration of particles in Batch B. While graphene has an extremely high thermal conductivity, diamond nanoparticles have a higher thermal conductivity than any of the particles found in Batch B. To cause a lower oil temperature, Batch B must have a higher concentration of particles, or provide much better friction reduction. From visual inspection, all of the Batch B oils had a higher concentration of

particles than Batch A. This would cause an improvement in heat transfer performance because all of the nanoparticles, especially diamond and graphene, have a much higher thermal conductivity than just the base oil.

Since Batch B.3 has the highest concentration of particles, it makes sense for it to provide the most heat transfer from the output side of the gearbox. The data, along with visual inspection of the oil, also suggests that this high concentration results in the oil being too thick to reliably flow through the input side of the gearbox. This may have increased friction, which caused the Input Duplex Bearing to increase in temperature. Batch B.2 resulted in lower temperatures than the Conventional oil at every thermocouple, but seemed to follow the same trend that is evident with Batch B.3. The IDB thermocouple measured the smallest temperature difference, while the thermocouples on the output side measured a larger temperature difference when compared to the conventional oil. Batch B.1 had the lowest nanoparticle concentration out of the Batch B oils and the data suggests that it causes the most uniform heat transfer. This is most likely due to the fact that the less viscous oil could flow throughout the gearbox with less resistance than the more concentrated Batch B oils.

These results agree with what was found by Gouda and Nasiri-Khuzani et al. The viscosities of the nano oils were higher than that of the base oil. The nano oils provided better friction reduction and heat transfer than the base oil. Like Gouda's tests, it was determined that at a certain point, excess particles can reduce performance. Batch A results can be compared to findings of Nasiri-Khuzani et al., because nanodiamond particles were used for both studies. Batch A did provide better heat transfer and lubrication performance than conventional oil, so this study helps to confirm the findings from the research

performed in tractor engines. The data cannot be directly compared to APU performance, however, because of the physical differences between a jet engine and a four stroke engine.

4.3 Auxiliary Power Unit

The main goal of this research is to determine if there are any benefits when using nano oils instead of Aeroshell 560 in the APU. The results show that there is an increase in efficiency for Batch A and Batch B. Batch A reduced the peak vibration by 35% and the RMS by 22%. The use of Batch B resulted in a 44% reduction in peak vibration and a 26% reduction in the RMS. This suggests that friction was reduced by a substantial amount. Vibration can result from contact of surface asperities during mixed-boundary lubrication and can be greatly reduced when an elastohydrodynamic regime occurs. This type of lubrication involves a compressible layer of oil that provides complete separation of the two surfaces. Oil with a higher viscosity usually results in a thicker boundary layer between surfaces. While this reduces friction between components, drag forces in the oil increase. The ideal lubricant should have the minimum viscosity required to provide an elastohydrodynamic regime throughout all operating conditions. The results suggest that both nano oils improve the fluid film, resulting in decreased vibration and increased efficiency.

The increase in temperature for Batch B oil is an unexpected outcome and requires additional testing to completely determine the cause. Increased friction usually causes increased vibration and heat. Batch B most likely reduced overall friction, because of the heat reduction in the IGB, the efficiency improvement in the APU, the vibration reduction in the APU, and the small engine results. This suggests that the higher APU oil temperature

was caused by another factor. There are several possible causes for the temperature increase. These include increased heat transfer from the combustor, a friction increase in only certain components, internal oil friction from nano particles of different densities and configurations, or decreased oil flow due to the clogged filter.

Increased heat transfer from other APU components, such as the combustion area, could be a cause of the temperature increase. No Load results show that Batch B provides excellent heat transfer. This is difficult to analyze with just the average run temperatures for the APU, so a transient comparison was performed. The average temperatures during the 15 to 45 minute portion of the runs are shown in Figure 3.9. The temperature of Batch B is increasing at a much higher rate than the other oils during the 15 to 28 minute portion of the tests. After this, the temperature begins to reach a steady state temperature while the temperature of the other oils continues to increase. A higher combustor temperature relates to increased efficiency. Less heat may be generated by friction, but more could be transferred from the rest of the engine. This suggests that Batch B is conducting heat much more efficiently than the other oils.
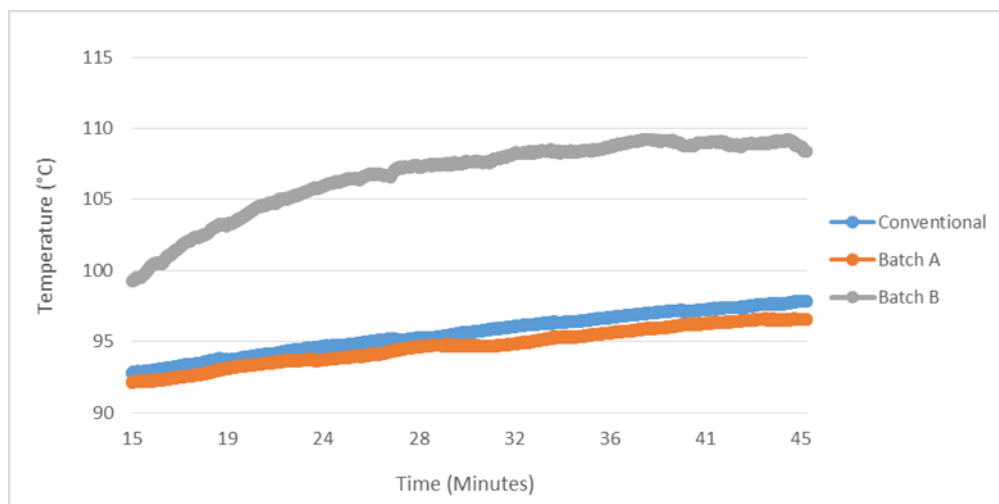
FIGURE 3.9 TRANSIENT APU OIL TEMPERATURE

The runs were not performed until steady state temperatures were reached for multiple reasons. The APU on an UH-60 usually runs for less than 30 minutes before takeoff. Analyzing steady-state data would not provide useful information for realistic scenarios. In addition to this, steady-state testing would require much longer runs and larger quantities of jet fuel. Figure 3.9 suggests that Batch B may lower friction, but also have a lower specific heat which causes its temperature to rise at a faster rate. The combustor may also be operating at a higher temperature because of reduced friction. The oil could get hotter due to this increase in temperature.

An increase in bearing friction along with a decrease in gear friction could also be a cause for the increased temperature. The study performed by Fernandes examined the effects of viscosity on gears and bearings. This showed that higher viscosity oils improved the efficiency of gears, while reducing the efficiency of bearings[5]. This is further confirmed by the fact that oils designed for only gear lubrication, such as AGL, have a much higher viscosity than turbine oils. Since Batch B has a higher viscosity than conventional oil, it may improve efficiency in the gear train. The efficiency of the bearings may be reduced because of drag forces associated with the more viscous lubricant. This could result in more heat generation.

There is little literature concerning the third possible cause for the higher oil temperature occuring with increased efficiency. Ruyek et al. consider nanoparticle size and mass while deterimining the drag forces, but didn't consider the effects of different particles flowing through the oil simultaneously. It was discovered that mass and volume affect the drag forces and that the forces are anisotropic[13]. Zinc sulfide, boron nitride,

and graphene have very different densities and shapes. The drag forces on each type of particle could vary by a large amount. The linear and centrifugal forces would not cause identical acceleration for different particle types. These particles may reduce friction between contacting surfaces, but could cause more friction within the fluid from the collision of nanoparticles.

The final theory provides the most likely cause of increased temperature for Batch B oil. The nano particle aggregations were measured with the optical microscope and found to be larger than 40 microns. The APU has an oil filter with 10 micron pores, so the clumps are caught in the filter. This is evident in Figure 3.10. The filter was changed between each type of oil. It begins to clog as it collects these particles, which results in a decrease in oil flow. If the flow rate of the oil is decreased, the heat from combustion would transfer out of the oil sump at a slower rate. This could cause Batch B to reach a higher temperature even though it has a higher thermal conductivity.
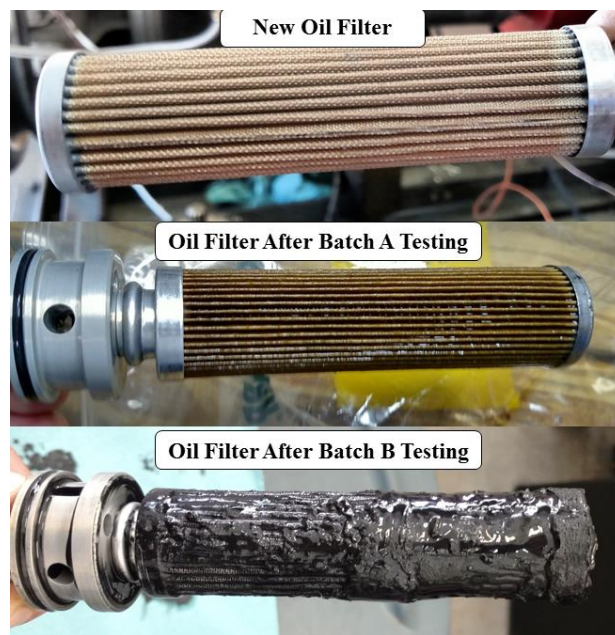
FIGURE 3.10 OIL FILTER BEFORE AND AFTER TESTING

The results show that there are promising benefits of using Batch A or Batch B oil instead of Aeroshell 560 in the APU. The nano oils need additional refinement before being considered ideal, but already provide some benefits. The clumping problems must be addressed before it could be considered for use in auxiliary power units during flight and the concentrations could be adjusted to provide optimal thermal conductivity and viscosity. Both oils provide overall efficiency improvements. While the reduction in fuel consumption is fairly small, it could provide a large cost savings when considered across an entire fleet of helicopters. Increasing the life of components by reducing wear could provide additional cost savings. If the oil filter clogging issue can be solved, switching to Batch B oil can improve APU performance.

4.4 Small Engine Test Stand

The efficiency and temperature improvements when using turbine oil instead of motor oil in the small engine are interesting and warrant further research, but the primary purpose of this study is to determine the effects of nanoparticle additives in base oils. The AeroShell and Penzoil comparison will be briefly discussed, but this section will primarily focus on the nano additive results.

One explanation for the increased efficiency and increased vibration is that there are multiple types of friction in a 4 stroke engine and the less viscous turbine oil may improve some types while making others worse. For instance, turbine oil may be viscous enough to maintain an elastohydrodynamic boundary layer between the piston and cylinder wall because the normal force acting on the cylinder wall by the motion of the piston is fairly small for a 5.5 hp engine and the force is primarily in the perpendicular direction.

The turbine oil may not provide sufficient lubrication for other components, such as between gear teeth and between the cams and valve stems. This could result in increased vibration and wear.

Based on the efficiency, temperature, and vibration results, Batch B.1 performed the best in the small engine. Efficiency improved by 0.6% over turbine oil and by 1.14% when compared to Pennzoil. Eventhough Batch B.1 increased APU oil temperature, it lowered the operating temperature of the oil in the small engine. It is worth noting that the small engine does not have an oil filter. This provides further evidence that it is more efficient at transferring heat and reducing friction than the conventional oil and that the APU temperature increase was caused by decreased oil flow because of the filter becoming clogged. The increase in efficiency and the large reduction in vibration suggest that Batch B.1 reduces friction throughout the small engine.

Batch A.2 and the Pennzoil with nanodiamond additives experienced similar results during small engine testing. Both decreased engine efficiency, decreased oil temperature, and had a small or negligible effect on vibration. The decrease in efficiency could be a result of the hard nano diamond particles being used in an application where a full boundary layer is already formed by just the base oil. These hard particles could cause scuffing on surfaces such as the piston or cylinder walls and a more significant increase in vibration would be noticable with extended testing. The nanodiamonds have a much higher thermal conductivity than the base oils, so any temperature increase due to friction could be negligible because of the increase in heat tranfer.

CHAPTER 5: CONCLUSION

This research compares two different types of nano oils and analyzes results from multiple tests to determine any benefits associated with using these oils as replacements for the conventional Aeroshell 560 turbine oil. This is performed by collecting fuel efficiency, temperature, and vibration data from the TRDT, No Load Test stand, APU Test Stand, and the Small Engine Test stand. Viscosity and particle size measurements are also collected and utilized while comparing the oils.

Batch A consists of nanodiamond particles suspended in Aeroshell 560 oil. The use of this oil resulted in a lower oil temperature during testing on the No Load Test Stand, but did not significantly affect oil temperature in the APU. It provided some improvement to fuel efficiency in the APU while greatly reducing vibration. These results suggest that Batch A does provide some benefits over the conventional oil.

Batch B contains zinc sulfide, boron nitride, and graphene nano particles. It caused the No Load Test Stand to operate at a much lower temperature than Batch A or conventional oil, but it resulted in a much higher oil temperature in the APU. While temperature greatly increased, vibration was substantially reduced. The use of Batch B in the APU and small engine resulted in the highest fuel efficiency for both tests. Because of

the increase in fuel efficiency and vibration reduction, the increased temperature is most likely not caused by an increase in friction. There are several explanations for this occurrence, but clogging of the oil filter is the most probable cause.

Both nano oils provide thermal and lubricating enhancements for the APU and IGB. Even though the current versions of the oils do not provide an exceptionally large increase in fuel efficiency, the results are promising and even a slight increase can provide substantial fuel cost savings if the oils are considered for fleet wide use in the APU and additional UH-60 components. The reduction in vibration can reduce component failures, which could reduce maintenance requirements and result in additional cost savings. The only concern with these oils comes from the images of large particle clumps and the large particle deposits on the APU oil filter. There is a possibility that clogging the filter could result in the APU overheating and automatically shutting down. In conclusion, both oils provide some benefits over conventional oil when used in the APU, but should be further optimized to improve nanoparticle suspension in the oil and to prevent particles from forming into large aggregates.

There are several future studies that could be performed to further this research. Some of these studies would expand upon the results of this research, while others can provide valuable information about additional UH-60 and AH-64 components and testing methods. These include: Batch B particle refinement then further testing to monitor oil filter clogging, a cost benefit analysis, tests to a CI change-out effects study, additional TRDT testing, modeling of the APU, and testing of additional concentrations and types of nano oils.

The clogging issue must be fixed before Batch B can be considered for use in an actual aircraft. Further testing, consisting of longer runs, should be performed with a refined Batch B oil to monitor this. A cost benefit analysis would provide a better understanding of the benefits associated with using these oils and would help to determine if the fuel efficiency increase would provide cost savings after considering the costs associated with adding nanoparticles to the conventional oil. During the TRDT portion of this research, it was determined that removing and reinstalling the IGB can result in large variations in temperature and CIs. Future work can be performed to further determine the effects of these change-outs and discover additional methods for avoiding variations in the results. In addition to this, further testing of Batch A and Batch B oils could be performed in the TRDT. This would provide additional data about the thermal and friction reducing properties of the oils. Additional research and APU testing could provide the opportunity to develop a computational model of the APU. Utilizing additional thermocouples and accelerometers while gathering data for various concentrations of oils, could provide enough information to create a model capable of predicting efficiency, temperature, and vibration results.

REFERENCES

[1]   Lee, Chang-Gun, Yu-Jin Hwang, Young-Min Choi, Jae-Keun Lee, Cheol Choi, and Je-Myung Oh. "A Study on the Tribological Characteristics of Graphite Nano Lubricants." International Journal of Precision Engineering and Manufacturing Int. J. Precis. Eng. Manuf. 10.1 (2009): 85-90. Web.

[2]   Hadi, Nazir Jawad, and Dhey Jawad Mohamed. The Effect of Nanoparticles on the Flow and Physical Behavior of Engine Lubricant Oil. Thesis. Collage of Materials Engineering /Polymer and Petrochemical Industry Department Babylon University/Iraq

[3]   Gouda, Kareem. "Application of Lubricants in the Ah-64d Helicopter Gearboxes for Improvement of Condition-based Maintenance Practices." Thesis. University of South Carolina, 2015.

[4]   Nasiri-Khuzani, Asoodar, Rahnama, and Rahnama. "Evaluation of Engine Parts Wear Using Nano Lubrication Oil in Agricultural Tractors Nano Lubrication." Global Journal of Science Frontier Research Agriculture and Veterinary Sciences 1st ser. 12.8 (2012)

[5]   FERNANDES, CARLOS MIGUEL DA COSTA GOMES. POWER LOSS IN ROLLING BEARINGS AND GEARS LUBRICATED WITH WIND TURBINE GEAR OILS. Thesis. DEPARTAMENTO DE ENGENHARIA MECÂNICA FACULDADE DE ENGENHARIA UNIVERSIDADE DO PORTO, 2015. Print.

[6]   Kakaras, E., A. Doukelis, A. Prelipceanu, and S. Karellas. "Inlet Air Cooling Methods for Gas Turbine Based Power Plants." J. Eng. Gas Turbines Power Journal of Engineering for Gas Turbines and Power 128.2 (2006): 312. Web.

[7]   Farouk, Naeim, Liu Sheng, and Qaisar Hayat. "Effect of Ambient Temperature on the Performance of Gas Turbines Power Plant." International Journal of Computer Science Issues 3rd ser. 10.1 (2013): n. pag. Web.

[8]   Sanders, Newell D. Performance Parameters for Jet-Propulsion Engines. Tech. no. 1106. 1946. Print.

[9]   "ECFR — Code of Federal Regulations." ECFR — Code of Federal Regulations. U.S. Government Publishing Office, Web. 09 Mar. 2016.

[10]   Wells-Brookfield Cone/Plate. Brookfield, n.d. Web. 22 Mar. 2016. <http://www.brookfieldengineering.com/products/viscometers/laboratory-wb-coneplate.asp>.

[11]   Edwards, Travis Steven. "METHODS FOR DETERMINING GREASE SERVICE LEVELS IN AN AH-64D INTERMEDIATE GEARBOX USING ON-BOARD SENSORS." Thesis. University of South Carolina, 2012.

[12]   Antolic, Lance J., and Jeremy S. Branning. Evaluation of Gear Condition Indicator Performance on Rotorcraft Fleet. Rep. Print.

[13]   Rudyak, Belkin, and Tomilina. Force Acting on a Nanoparticle in a Fluid. Rep. N.p.: Pleiades, 2008. Print

[14]   Seireg, Ali. Friction and Lubrication in Mechanical Design. New York: Marcel Dekker, 1998. Print.

[15]   Gas Turbine Engine Auxiliary Power Unit T-62T-40-1. Tech. no. TM 1-2835-208-23&P.
           Print.

[16]   Kanniah, Vinod, "0 CHARACTERIZATION" (2012). Theses and Dissertations--
           Chemical and Materials Engineering. Paper 8.

APPENDIX A: RSTUDIO SAMPLE CODE

An example of RStudio code is shown below. The first line imports the data. The second creates a boxplot of the data. The third line loads the data from specific columns in the file. The summary command provides some basic information about the data. The TukeyHSD code finds the difference between the data sets and the p value associated with each comparison.

```
> data <- read.csv(file.choose(),header=TRUE)
> boxplot(data$Eff~data$Type)
> Eff.aov <- aov(data$Eff~data$Type)
> summary(Eff.aov)
               Df Sum Sq Mean Sq F value Pr(>F)
data$Type       2  126.9   63.44    7865 <2e-16 ***
Residuals   31166  251.4    0.01
---
Signif. codes:
0 '***' 0.001 '**' 0.01 '*' 0.05 '.' 0.1 ' ' 1
>
> TukeyHSD(Eff.aov,conf.level=0.95)
  Tukey multiple comparisons of means
    95% family-wise confidence level

Fit: aov(formula = data$Eff ~ data$Type)

$`data$Type`
                   diff         lwr         upr
BatchB-BatchA  0.09788425  0.09503519  0.10073331
conv-BatchA   -0.05837177 -0.06133209 -0.05541144
conv-BatchB   -0.15625602 -0.15923062 -0.15328141
              p adj
BatchB-BatchA     0
conv-BatchA       0
conv-BatchB       0
```

FIGURE A.1 SAMPLE RSTUDIO CODE

58

APPENDIX B: SAMPLES OF DATA

Excerpts of data for the TRDT, No Load, and APU testing are provided here.

TABLE B.1 SAMPLE OF APU OIL TEMPERATURE DATA

Time(s)	Time(min)			Conventional Oil Run 1				
				Oil Temp(°F)	Oil Temp(°C)	Ambient Temp (°C)	Ambient Temp (°F)	Corrected Temp(°F)
900	15			153.684431	67.60246167	13.33333333	56	197.684431
900.2	15.00333			153.691388	67.60632667	13.33333333	56	197.691388
900.4	15.00667			153.691388	67.60632667	13.33333333	56	197.691388
900.6	15.01			153.726621	67.62590056	13.33333333	56	197.726621
900.8	15.01333			153.706134	67.61451889	13.33333333	56	197.706134
901	15.01667			153.705795	67.61433056	13.33333333	56	197.705795
901.2	15.02			153.704965	67.61386944	13.33333333	56	197.704965
901.4	15.02333			153.710089	67.61671611	13.33333333	56	197.710089
901.6	15.02667			153.744737	67.635965	13.33333333	56	197.744737
901.8	15.03			153.748972	67.63831778	13.33333333	56	197.748972
902	15.03333			153.733986	67.62999222	13.33333333	56	197.733986
902.2	15.03667			153.747143	67.63730167	13.33333333	56	197.747143
902.4	15.04			153.753061	67.64058944	13.33333333	56	197.753061
902.6	15.04333			153.761569	67.64531611	13.33333333	56	197.761569
902.8	15.04667			153.744522	67.63584556	13.33333333	56	197.744522

TABLE B.2 SAMPLE OF APU EFFICIENCY DATA

Time(S)	Time(min)	Fuel Flow(mL/s)	Hp	Brake (RPM)	Torque (ft-lb)	Energy Density (MJ/L)	Efficiency	A-Temp	Humidity	A-Temp	Barometric Pressure
900.0005	15.000008	13.104348	33.65	12023	14.7	35.3	5.424492194	67	68.91	19.44444	30.51
			33.64	12023	14.69			67	68.91	19.44444	30.51
			33.64	12024	14.69			67	68.91	19.44444	30.51
			33.65	12024	14.7			67	68.91	19.44444	30.51
			33.69	12024	14.72			67	68.91	19.44444	30.51
			33.76	12024	14.75			67	68.91	19.44444	30.51
			33.84	12023	14.78			67	68.9	19.44444	30.51
			33.9	12022	14.81			67	68.9	19.44444	30.51
			33.94	12022	14.83			67	68.9	19.44444	30.51
			33.96	12021	14.84			67	68.9	19.44444	30.51
901.0005	15.016676	13.121739	33.95	12021	14.84		5.465599705	67	68.9	19.44444	30.51
			33.93	12021	14.82			67	68.9	19.44444	30.51
			33.88	12021	14.8			67	68.89	19.44444	30.51
			33.83	12021	14.78			67	68.89	19.44444	30.51
			33.8	12021	14.77			67	68.89	19.44444	30.51
			33.78	12021	14.76			67	68.89	19.44444	30.51
			33.77	12021	14.75			67	68.89	19.44444	30.51
			33.74	12021	14.74			67	68.89	19.44444	30.51
			33.72	12021	14.73			67	68.89	19.44444	30.51
			33.69	12022	14.72			67	68.89	19.44444	30.51
902.0006	15.033343	13.156522	33.68	12023	14.71		5.407797544	67	68.89	19.44444	30.51

TABLE B.3 SAMPLE OF NO LOAD DATA

odb	irb	orb	idb	type
159.7204	160.973	151.983	169.2541	conv
159.7204	160.973	151.983	169.2541	conv
159.7575	160.9464	151.981	169.2446	conv
159.7575	160.9464	151.981	169.2446	conv
159.7685	160.951	152.0215	169.2529	conv
159.7685	160.951	152.0215	169.2529	conv
159.7409	160.962	152.0258	169.2459	conv
159.7409	160.962	152.0258	169.2459	conv
159.7729	160.9737	152.0375	169.3073	conv
159.7729	160.9737	152.0375	169.3073	conv
159.7791	161.042	152.0698	169.3457	conv
159.7791	161.042	152.0698	169.3457	conv
159.8019	160.9919	152.0343	169.3061	conv
159.8019	160.9919	152.0343	169.3061	conv

Conventional					
Run 1	**Temp (° F)**	**Input FM4**	**Output FM4**	**Input DA1**	**Output DA1**
Mean	212.5045	3.2262	2.90015	7.3087	7.17975
Standard Deviation	1.529514801	0.313698078	0.109835415	0.167423227	0.176049298
Variance	2.339415526	0.098406484	0.012063818	0.028030537	0.030993355
Margin of Error	1.123310441	0.047251559	0.005792649	0.013459342	0.01488199
% Error	0.528605484	1.464619651	0.199736189	0.184155082	0.20727728
Run 2	**Temp (° F)**	**Input FM4**	**Output FM4**	**Input DA1**	**Output DA1**
Mean	211.6857	3.2304	2.9323	7.37065	7.2194
Standard Deviation	2.345027283	0.231203123	0.148893498	0.243208439	0.201860139
Variance	5.499152958	0.053454884	0.022169274	0.059150345	0.040747516
Margin of Error	2.640512499	0.025667278	0.010644957	0.028402051	0.019565618
% Error	1.247374054	0.794554185	0.363024129	0.385339846	0.271014458
Run 3	**Temp (° F)**	**Input FM4**	**Output FM4**	**Input DA1**	**Output DA1**
Mean	210.7535	3.3646	2.88655	7.305	7.12655
Standard Deviation	3.304377121	0.287054992	0.177119786	0.13681605	0.126653475
Variance	10.91890816	0.082400568	0.031371418	0.018718632	0.016041103
Margin of Error	5.242900804	0.039566045	0.015063524	0.008988072	0.00770241
% Error	2.48769335	1.175950916	0.521852176	0.123039995	0.108080491
Run 4	**Temp (° F)**	**Input FM4**	**Output FM4**	**Input DA1**	**Output DA1**
Mean	209.868	3.57665	2.9123	6.7788	6.5809
Standard Deviation	3.159036495	0.240913672	0.133428909	0.255468939	0.235765919
Variance	9.979511579	0.058039397	0.017803274	0.065264379	0.055585568
Margin of Error	4.791833444	0.027868611	0.008548547	0.03133781	0.026690363
% Error	2.283260642	0.779181942	0.293532495	0.462291403	0.405573142
Run 5	**Temp (° F)**	**Input FM4**	**Output FM4**	**Input DA1**	**Output DA1**
Mean	212.1305	3.33245	2.95665	6.70145	6.48795
Standard Deviation	2.445585658	0.368687498	0.159587387	0.203540886	0.201806962
Variance	5.980889211	0.135930471	0.025468134	0.041428892	0.04072605
Margin of Error	2.871826413	0.065269344	0.012228961	0.019892792	0.019555311
% Error	1.353801746	1.958599358	0.413608677	0.296843105	0.301409699

TABLE B.5 CONVENTIONAL APU EFFICIENCY DATA

Run 1					
	Fuel Flow(mL/s)	Hp (Hp)	Brake (RPM)	Torque (ft-lb)	Efficiency
Mean	13.1137	34.0050	12022.3173	14.8556	5.4782
Standard Deviation	0.1105	0.2453	5.9897	0.1124	0.0602
Variance	0.0122	0.0602	35.8760	0.0126	0.0036
n	1800	17991	17991	17991	1800
df	1799	17990	17990	17990	1799
t statistic (df) (95%)	1.96	1.96	1.96	1.96	1.96
Margin of Error	0.0006	0.0009	0.5243	0.0002	0.0002
% Error	0.0043%	0.0026%	0.0044%	0.0012%	0.0031%
Run 2					
	Fuel Flow(mL/s)	Hp (Hp)	Brake (RPM)	Torque (ft-lb)	Efficiency
Mean	13.1879	33.8065	12024.1884	14.7665	5.4157
Standard Deviation	0.1181	0.1856	3.2003	0.0818	0.0555
Variance	0.0140	0.0345	10.2420	0.0067	0.0031
n	1777	17761	17761	17761	1777
df	1776	17760	17760	17760	1776
t statistic (df) (95%)	1.96	1.96	1.96	1.96	2.96
Margin of Error	0.0006	0.0005	0.1506	0.0001	0.0002
% Error	0.0049%	0.0015%	0.0013%	0.0007%	0.0040%
Run 3					
	Fuel Flow(mL/s)	Hp (Hp)	Brake (RPM)	Torque (ft-lb)	Efficiency
Mean	12.8992	34.0443	12009.5384	14.8886	5.5758
Standard Deviation	0.1269	0.1998	6.1996	0.0924	0.0625
Variance	0.0161	0.0399	38.4349	0.0085	0.0039
n	1800	18000	18000	18000	1800
df	1799	17999	17999	17999	1799
t statistic (df) (95%)	1.96	1.96	1.96	1.96	2.96
Margin of Error	0.0007	0.0006	0.5615	0.0001	0.0003
% Error	0.0058%	0.0017%	0.0047%	0.0008%	0.0049%
Run 4					
	Fuel Flow(mL/s)	Hp (Hp)	Brake (RPM)	Torque (ft-lb)	Efficiency
Mean	12.7359	33.5821	11998.1394	14.7004	5.5707
Standard Deviation	0.1397	0.2301	6.3737	0.1041	0.0653
Variance	0.0195	0.0530	40.6240	0.0108	0.0043
n	1800	18001	18001	18001	1800
df	1799	18000	18000	18000	1799
t statistic (df) (95%)	7.96	1.96	1.96	1.96	2.96
Margin of Error	0.0037	0.0008	0.5935	0.0002	0.0003
% Error	0.0288%	0.0023%	0.0049%	0.0011%	0.0053%

Run 5					
	Fuel Flow(mL/s)	**Hp (Hp)**	**Brake (RPM)**	**Torque (ft-lb)**	**Efficiency**
Mean	12.7245	33.8061	11987.6831	14.8114	5.6129
Standard Deviation	0.1432	0.3334	8.2640	0.1539	0.0793
Variance	0.0205	0.1112	68.2930	0.0237	0.0063
n	1800	18001	18001	18001	1800
df	1799	18000	18000	18000	1799
t statistic (df) (95%)	7.96	1.96	1.96	1.96	2.96
Margin of Error	0.0038	0.0016	0.9977	0.0003	0.0004
% Error	0.0302%	0.0048%	0.0083%	0.0023%	0.0078%
Run 6					
	Fuel Flow(mL/s)	**Hp (Hp)**	**Brake (RPM)**	**Torque (ft-lb)**	**Efficiency**
Mean	12.9776	33.7818	12018.5534	14.7627	5.4994
Standard Deviation	0.1319	0.1704	3.8337	0.0765	0.0577
Variance	0.0174	0.0290	14.6975	0.0059	0.0033
n	1800	18001	18001	18001	1800
df	1799	18000	18000	18000	1799
t statistic (df) (95%)	1.96	1.96	1.96	1.96	2.96
Margin of Error	0.0008	0.0004	0.2147	0.0001	0.0002
% Error	0.0062%	0.0013%	0.0018%	0.0006%	0.0042%
Run 7					
	Fuel Flow(mL/s)	**Hp (Hp)**	**Brake (RPM)**	**Torque (ft-lb)**	**Efficiency**
Mean	12.8617	33.8569	12006.9476	14.8098	5.5613
Standard Deviation	0.1418	0.3294	6.6001	0.1510	0.0737
Variance	0.0201	0.1085	43.5609	0.0228	0.0054
n	1800	18001	18001	18001	1800
df	1799	18000	18000	18000	1799
t statistic (df) (95%)	1.96	1.96	1.96	1.96	2.96
Margin of Error	0.0009	0.0016	0.6364	0.0003	0.0004
% Error	0.0072%	0.0047%	0.0053%	0.0022%	0.0068%

TABLE B.6 BATCH A APU DATA

Batch A Run 1					
	Fuel Flow(mL/s)	**Hp (Hp)**	**Brake (RPM)**	**Torque (ft-lb)**	**Efficiency**
Mean	12.7989	33.8904	11997.5960	14.8360	5.5941
Standard Deviation	0.1362	0.2042	5.5552	0.0940	0.0678
Variance	0.0185	0.0417	30.8606	0.0088	0.0046
n	1800	18001	18001	18001	1800
df	1799	18000	18000	18000	1799
t statistic (df) (95%)	1.96	1.96	1.96	1.96	1.96
Margin of Error	0.0009	0.0006	0.4508	0.0001	0.0002
% Error	0.0067%	0.0018%	0.0038%	0.0009%	0.0038%
Batch A Run 2					
	Fuel Flow(mL/s)	**Hp (Hp)**	**Brake (RPM)**	**Torque (ft-lb)**	**Efficiency**
Mean	12.9734	33.7006	12017.1163	14.7289	5.4876
Standard Deviation	0.0439	0.2561	5.6623	0.1165	0.0415
Variance	0.0019	0.0656	32.0612	0.0136	0.0017
n	1800	18001	18001	18001	1800
df	1799	18000	18000	18000	1799
t statistic (df) (95%)	1.96	1.96	1.96	1.96	1.96
Margin of Error	0.0001	0.0010	0.4684	0.0002	0.0001
% Error	0.0007%	0.0028%	0.0039%	0.0013%	0.0015%
Batch A Run 3					
	Fuel Flow(mL/s)	**Hp (Hp)**	**Brake (RPM)**	**Torque (ft-lb)**	**Efficiency**
Mean	12.7755	33.8669	12004.9126	14.8168	5.6001
Standard Deviation	0.0486	0.2830	7.4557	0.1312	0.0472
Variance	0.0024	0.0801	55.5876	0.0172	0.0022
n	1800	18001	18001	18001	1800
df	1799	18000	18000	18000	1799
t statistic (df) (95%)	1.96	1.96	1.96	1.96	1.96
Margin of Error	0.0001	0.0012	0.8121	0.0003	0.0001
% Error	0.0009%	0.0035%	0.0068%	0.0017%	0.0018%
Batch A Run 4					
	Fuel Flow(mL/s)	**Hp (Hp)**	**Brake (RPM)**	**Torque (ft-lb)**	**Efficiency**
Mean	12.5847	33.8699	11985.6532	14.8418	5.6856
Standard Deviation	0.0742	0.1793	6.2165	0.0842	0.0479
Variance	0.0055	0.0322	38.6445	0.0071	0.0023
n	1795	17941	17941	17941	1795
df	1794	17940	17940	17940	1794
t statistic (df) (95%)	1.96	1.96	1.96	1.96	1.96
Margin of Error	0.0003	0.0005	0.5655	0.0001	0.0001
% Error	0.0020%	0.0014%	0.0047%	0.0007%	0.0019%

Batch A Run 5					
	Fuel Flow(mL/s)	Hp (Hp)	Brake (RPM)	Torque (ft-lb)	Efficiency
Mean	12.7278	33.5998	11994.5039	14.7127	5.5774
Standard Deviation	0.1195	0.2576	8.8511	0.1194	0.0631
Variance	0.0143	0.0664	78.3411	0.0143	0.0040
n	1800	18001	18001	18001	1800
df	1799	18000	18000	18000	1799
t statistic (df) (95%)	1.96	1.96	1.96	1.96	1.96
Margin of Error	0.0007	0.0010	1.1445	0.0002	0.0002
% Error	0.0052%	0.0029%	0.0095%	0.0014%	0.0033%
Batch A Run 6					
	Fuel Flow(mL/s)	Hp (Hp)	Brake (RPM)	Torque (ft-lb)	Efficiency
Mean	12.7508	33.6659	12008.8796	14.7239	5.5781
Standard Deviation	0.1161	0.1280	6.0302	0.0564	0.0503
Variance	0.0135	0.0164	36.3632	0.0032	0.0025
n	1761	17601	17601	17601	1761
df	1760	17600	17600	17600	1760
t statistic (df) (95%)	1.96	1.96	1.96	1.96	1.96
Margin of Error	0.0006	0.0002	0.5372	0.0000	0.0001
% Error	0.0049%	0.0007%	0.0045%	0.0003%	0.0021%
Batch A Run 7					
	Fuel Flow(mL/s)	Hp (Hp)	Brake (RPM)	Torque (ft-lb)	Efficiency
Mean	12.6621	33.7052	11991.5797	14.7623	5.6231
Standard Deviation	0.0629	0.2072	5.8441	0.0942	0.0394
Variance	0.0040	0.0429	34.1540	0.0089	0.0015
n	1800	18001	18001	18001	1800
df	1799	18000	18000	18000	1799
t statistic (df) (95%)	1.96	1.96	1.96	1.96	1.96
Margin of Error	0.0002	0.0006	0.4990	0.0001	0.0001
% Error	0.0014%	0.0019%	0.0042%	0.0009%	0.0013%

TABLE B.7 BATCH B APU DATA

Batch B Run 1					
	Fuel Flow(mL/s)	Hp (Hp)	Brake (RPM)	Torque (ft-lb)	Efficiency
Mean	12.7043	33.7607	12012.4488	14.7610	5.6143
Standard Deviation	0.1223	0.2076	6.9954	0.0968	0.0606
Variance	0.0150	0.0431	48.9354	0.0094	0.0037
n	1801	18001	18001	18001	1800
df	1800	18000	18000	18000	1799
t statistic (df) (95%)	1.96	1.96	1.96	1.96	1.96
Margin of Error	0.0007	0.0006	0.7149	0.0001	0.0002
% Error	0.0054%	0.0019%	0.0060%	0.0009%	0.0030%
Batch B Run 2					
	Fuel Flow(mL/s)	Hp (Hp)	Brake (RPM)	Torque (ft-lb)	Efficiency
Mean	12.5519	33.6597	12006.2587	14.7245	5.6656
Standard Deviation	0.1502	0.4246	11.1120	0.1955	0.0973
Variance	0.0226	0.1803	123.4761	0.0382	0.0095
n	1785	17841	17841	17841	1785
df	1784	17840	17840	17840	1784
t statistic (df) (95%)	1.96	1.96	1.96	1.96	1.96
Margin of Error	0.0010	0.0026	1.8119	0.0006	0.0004
% Error	0.0083%	0.0079%	0.0151%	0.0038%	0.0078%
Batch B Run 3					
	Fuel Flow(mL/s)	Hp (Hp)	Brake (RPM)	Torque (ft-lb)	Efficiency
Mean	12.3891	34.0930	11968.9670	14.9604	5.8134
Standard Deviation	0.0653	0.1666	8.0945	0.0794	0.0416
Variance	0.0043	0.0278	65.5215	0.0063	0.0017
n	1801	18001	18001	18001	1801
df	1800	18000	18000	18000	1800
t statistic (df) (95%)	1.96	1.96	1.96	1.96	1.96
Margin of Error	0.0002	0.0004	0.9572	0.0001	0.0001
% Error	0.0016%	0.0012%	0.0080%	0.0006%	0.0014%
Batch B Run 4					
	Fuel Flow(mL/s)	Hp (Hp)	Brake (RPM)	Torque (ft-lb)	Efficiency
Mean	12.7286	33.8386	12010.5323	14.7974	5.6166
Standard Deviation	0.1104	0.1685	6.8916	0.0788	0.0558
Variance	0.0122	0.0284	47.4940	0.0062	0.0031
n	1801	18001	18001	18001	1801
df	1800	18000	18000	18000	1800
t statistic (df) (95%)	1.96	1.96	1.96	1.96	1.96
Margin of Error	0.0006	0.0004	0.6938	0.0001	0.0001
% Error	0.0044%	0.0012%	0.0058%	0.0006%	0.0026%

Batch B Run 5					
	Fuel Flow(mL/s)	**Hp (Hp)**	**Brake (RPM)**	**Torque (ft-lb)**	**Efficiency**
Mean	12.4767	33.6261	11989.5893	14.7302	5.6934
Standard Deviation	0.0595	0.3245	10.0074	0.1500	0.0547
Variance	0.0035	0.1053	100.1490	0.0225	0.0030
n	1801	18001	18001	18001	1801
df	1800	18000	18000	18000	1800
t statistic (df) (95%)	1.96	1.96	1.96	1.96	1.96
Margin of Error	0.0002	0.0015	1.4631	0.0003	0.0001
% Error	0.0013%	0.0046%	0.0122%	0.0022%	0.0024%
Batch B Run 6					
	Fuel Flow(mL/s)	**Hp (Hp)**	**Brake (RPM)**	**Torque (ft-lb)**	**Efficiency**
Mean	12.2860	33.6795	11970.9832	14.7764	5.7911
Standard Deviation	0.0601	0.0582	9.2657	0.0331	0.0302
Variance	0.0036	0.0034	85.8526	0.0011	0.0009
n	1801	18001	18001	18001	1801
df	1800	18000	18000	18000	1800
t statistic (df) (95%)	1.96	1.96	1.96	1.96	1.96
Margin of Error	0.0002	0.0000	1.2542	0.0000	0.0000
% Error	0.0014%	0.0001%	0.0105%	0.0001%	0.0007%
Batch B Run 7					
	Fuel Flow(mL/s)	**Hp (Hp)**	**Brake (RPM)**	**Torque (ft-lb)**	**Efficiency**
Mean	12.3508	33.2087	11971.3484	14.5696	5.6799
Standard Deviation	0.1404	0.6488	8.6274	0.2915	0.1005
Variance	0.0197	0.4209	74.4322	0.0850	0.0101
n	1801	18001	18001	18001	1801
df	1800	18000	18000	18000	1800
t statistic (df) (95%)	1.96	1.96	1.96	1.96	1.96
Margin of Error	0.0009	0.0061	1.0874	0.0012	0.0005
% Error	0.0074%	0.0185%	0.0091%	0.0085%	0.0086%

APPENDIX C: SENSOR ACCURACY

TABLE C.1 ACCURACY OF SENSORS

Sensor	Accuracy
Thermocouples	± 0.4%
Accelerometers	± 5.0%
Fuel Flow Meter	± 0.2%
Water Brake Torque	± 0.5% FS